American Journal of
Biomedical Science & Research

www.biomedgrid.com
ISSN: 2642-1747

Review Article

Copyright © All rights are reserved by CAC Sequeira

Membrane Electrolytes for PEMFCs

CAC Sequeira[1*] and Tiago AR Silva[2]

[1]*Department of Chemical Engineering, Instituto Superior Técnico, University of Lisbon, Av. Rovisco Pais, 1049-001 Lisbon, Portugal*

[2]*Centro de Química Estrutural, CQE, Instituto Superior Técnico, University of Lisbon, Av. Rovisco Pais, 1049-001 Lisboa, Portugal*

***Corresponding author:** CAC Sequeira, Department of Chemical Engineering, Instituto Superior Técnico, University of Lisbon, Av. Rovisco Pais, 1049-001 Lisbon, Portugal.

To Cite This article: *CAC Sequeira* and Tiago AR Silvab, Membrane Electrolytes for PEMFCs. Am J Biomed Sci & Res. 2026 32(2) AJBSR. MS.ID.004141,* **DOI:** 10.34297/AJBSR.2026.32.004141

Received: August 17, 2026 **Published:** September 11, 2026

Abstract

The present paper addresses the basics of PEMFC (proton exchange membrane fuel cell) for transport applications, pointing out the advantages and difficulties encountered in their development. Cell components are briefly considered and their requirements for the successful introduction of the PEMFC are also analyzed. Main membrane electrolytes for the MEAs are really at the heart of the fuel cell, being one of their major components, and fundamental and applied investigations of them conducted during the last years, are emphasized in the present review.

Keywords: Proton Exchange Membrane Fuel Cells, Membrane Electrolytes, Nafion, Composite Membranes, Blend/Hybrid Membranes, Fuel Cell Vehicles, Green Hydrogen

Introduction

A large part of the world`s oil production is consumed by petrol and diesel engines [1]. When fossil fuels are burned, they release large amounts of carbon dioxide into the air, and this and other greenhouse gases produced by the fossil oil trap in our atmosphere originate global warming. Therefore, sustainable energy sources are urgently required for the transportation sector of the economy. Electricity is the most direct way of utilizing renewable energy, thus switching to electric propulsion seems to be an excellent approach, by alleviating the present pollution from Internal-Combustion-Engine Vehicles (ICEVs) and by providing silent power for transportation. But most renewable sources of energy are intermittent, opening spatial and temporal gaps between the availability of the energy and its consumption by the end-users [2]. Hence, it is necessary to develop suitable electrochemical energy conversion and storage systems, such as PEMFCs.

Depending on the source of the electrical power [3], five electric and hybrid versions of passenger and goods vehicles can be established:

a) Tramcars and trolleybuses, electric trains, and urban metro systems, which are supplied directly by mains electricity.

b) Railway locomotives and ships in which a diesel engine drives a generator to supply electricity to a motor.

c) Battery Electric vehicles (BEVs), gaining interest in battery electric cars and vans for urban use.

d) Hybrid Electric vehicles (HEVs), with dual power sources, one being electric.

e) Fuel-Cell Vehicles (FCVs), with current interest among the automotive companies for providing electricity for motive power.

This work is licensed under Creative Commons Attribution 4.0 License

In recent years the technology of fuel cells, particularly Polymer Electrolyte Fuel Cells (PEMFCs), has become one of the most innovative areas of science and engineering. Industrial initiatives, publicly funded R&D programs, and academic activities have created a broad base of competence in materials research, cell, stack, and system developments. Fuel concepts based on hydrogen, methanol, reformed hydrocarbons, etc. are evaluated, and concepts for commercialization are introduced. Therefore, the PEMFC technology has an impressive market opportunity for applications such as portable stationary, and mobile power sources. Small fuel cells may be used to provide portable electronic devices with long-duration electric power. They may be integrated into vacuum cleaners or lawn mowers, making these electric appliances cordless and more convenient to operate. Bicycles and scooters may be supplied with clean and quiet fuel cell power sources. Certainly, the family car is another important application for fuel cells. Buses equipped with fuel cell power sources are coming into daily service in several cities in Europe and other parts of the world. Another important application is distributed co-generation. Fuel cell co-generators are becoming the home source of heat and power.

When hydrogen is stored as renewable energy, it needs to be reconverted to electricity, which happens in a fuel cell. This is essentially a water electrolyze working in reverse; a fuel gas (usually hydrogen) is fed to the negative electrode and oxygen (or air) to the positive electrode [4]. The hydrogen-oxygen fuel cell is theoretically the best fuel cell one could devise. The theoretical energy density is 3.66 kWh kg^{-1} counting the weight of both hydrogen and oxygen. This should be compared to the values of 170 Wh /kg and 265 Wh /kg calculated for the lead/acid and lithium-ion batteries, respectively. However, this number is misleading, because it is calculated only by the weight of the fuel and the oxidant, ignoring the weight of the fuel container. The energy density of molecular hydrogen is the highest of all elements, but in any method of storing it, the weight of the container is at least 10 times the weight of the hydrogen contained in it. It could be argued that the energy stored in the fuel cell proper approaches zero, while the energy of a fuel cell system approaches asymptotically the energy density of the fuels and their containers. For space applications, both hydrogen and oxygen are carried cryogenically (as the corresponding liquids) hence the energy density of the system has to include the containers of both gases. For terrestrial applications, a hydrogen-air fuel cell would be preferred, alleviating the need to store oxygen. Nevertheless, the cost of the electrode materials, the safety aspects of storing hydrogen, and the low density of stored hydrogen, either as a compressed gas or cryogenically, have so far prevented this type of fuel cell from becoming widely used, although it has been employed successfully in space missions.

Oxidation of fuel is one of the problems of fuel cells. The other is the reduction of oxygen. In an acid solution, the open circuit potential for oxygen reduction should be 1.23 V vs. RHE, but in effect, it is about 1.0 V. This already reduces the efficiency of energy conversion to about 80%. Moreover, the reduction of oxygen is a relatively slow process, so a further loss of efficiency will result from the charge transfer overpotential. To be viable, a fuel cell should operate at a high current density, of the order of 1 A cm^{-2}, hence even a small ohmic resistance between the two electrodes may cause a significant loss of efficiency of energy conversion. This requires optimization of the thickness of the electrolyte membrane (e.g., Nafion) for low resistivity combined with low permeability for methanol. It should be mentioned at this point, that Nafion (baseline perfluorinated ionomers) and its modified membranes (e.g., copolymer, blended, composite membranes) are being largely investigated and applied in several sectors, namely in the car industry. The methanol fuel cell, considered in general as a type of PEMFC, can reform methanol into hydrogen, which in turn powers the hydrogen/oxygen fuel cell, with all this happening onboard the electric vehicle. A major obstacle to this fuel cell is the methanol crossover, which is related to the cell membrane. Particularly, the methanol concentration, the cell temperature, and the membrane thickness have a considerable effect on methanol crossover. The cell performance, either for the PEMFC or the methanol fuel cell, is largely dependent on the protonic conductivity and the low permeability (permselectivity) for methanol [5,6].

A further difficulty is that reduction of molecular oxygen could easily lead to the 2-electron reduction to hydrogen peroxide instead of the 4-electron reduction to water or OH^-. In Low-Temperature (LT) or Intermediary Temperature (IT) fuel cells, if the hydrogen ion is the conducting species, then water is formed at the oxygen electrode; conversely, in Alkaline Anion Exchange Membrane Fuel Cells (AAEMFCs), working at LT, in which the fuel, hydrogen or methanol, is supplied at the anode and oxygen from the air, and water is supplied to the cathode. Then at the cathode electrode, oxygen reduction produces hydroxide ions that migrate through the electrolyte toward the anode. At the anode, hydroxide ions react with the fuel to produce water and electrons [7].

Electrons go through the circuit producing current. The global electrochemical reaction when hydrogen or methanol is the fuel is identical to the global reaction for the PEMFC. In HT fuel cells (e.g., solid oxide fuel cells), the cathode process (the air electrode) normally involves the reduction of molecular oxygen to oxygen anions using electrons external to the cell, and the formed oxide ions are transported through the ionically conducting (but electronically insulating) solid electrolyte to the anode where they react electrochemically with the fuel gas, originating water [8]. If hydrogen is the fuel, the overall process is identical to the overall process of the PEMFC at LT. A fuel cell differs from a conventional battery in that the reactants, in general, are gaseous and the chemical energy is stored in an outside container, rather than inside the battery. Therefore, the capacity of the cell device is limited only by the size of the fuel and oxidant supply and not by the cell design. For this reason, fuel cells are rated by their power output (kW) rather than by their capacity (kWh). This can be a great advantage from the point of view of energy density since, for extended operation, the weight of the cell itself is insignificant.

The fuel cell was invented in 1839 by Sir William Grove and therefore pre-dated the first internal-combustion engines by about 50 years. Its perceived advantages for power generation, namely high thermodynamic efficiency, high energy efficiency, low operating temperature, good performance under low-load conditions, silent operation, low pollution emission, simplicity of design, and molecular factory construction, led to its great investigation. Against these advantages must be set the many difficulties that have been encountered in the attempts to bring fuel cells to commercial realization [9,10], namely their high cost, low power density, and low durability. The primary fuels of natural gas, oil, and coal must first be reformed to hydrogen, and the difficulty of developing a fully satisfactory reformer is comparable to the difficulty of developing the fuel cell itself [11-14].

There are six principal types of fuel cells, as summarized in (Table 1). Their mode of operation is illustrated in (Figure 1). This fuel cells fall into three broad categories as regards their temperature of operation:

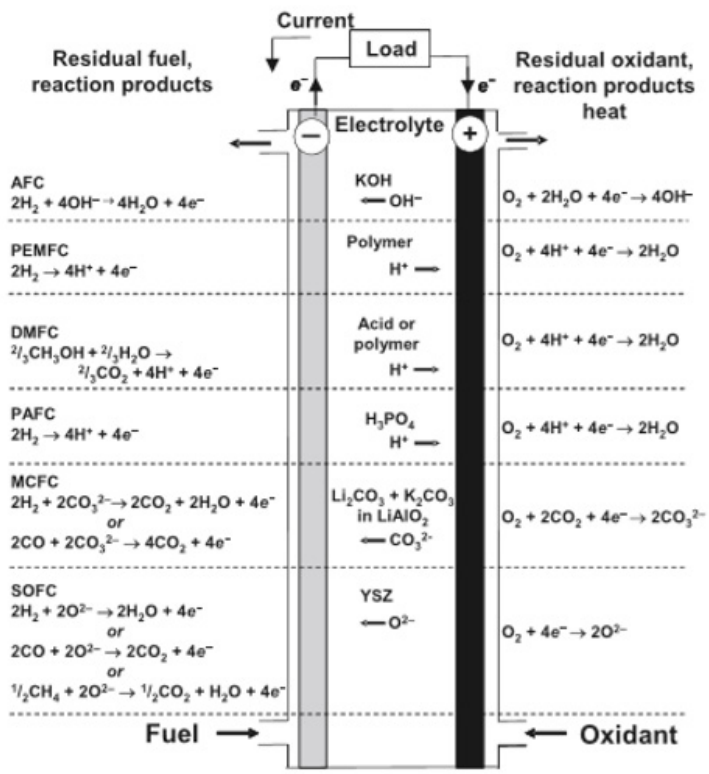

Figure 1: Electrochemical reactions occurring in different types of fuel cells.

Table 1: Principal Types of Fuel Cell.

Fuel-cell technology[a]	Electrolyte	Temperature Range (ºC)	Electrocatalyst		Fuel	Efficiency[b] (% HHV)	Start-up time (h)
			Positive Electrode	Negative Electrode			
PAFC	H_3PO_4	150 - 220	Pt supported on C	Pt supported on C	H_2 (low S, low CO, tolerant to CO_2)	35 - 45	4-Jan
AFC	KOH	50 - 150	NiO, Ag, or Au-Pt	Ni, steel, or Pt-Pd	Pure H_2	45 - 60	< 0.1
PEMFC	Polymer[c]	80 - 90	Pt supported on C	Pt supported on C	Pure H_2	40 - 60	< 0.1
DMFC	H_2SO_4 Polymer[c]	60 - 90	Pt supported on C	Pt supported on C Pt-Ru	CH_3OH	35 - 40	< 0.1

MCFC	Li_2CO_3	600 -700	Lithiated NiO	Sintered Ni-Cr and Ni-Al alloys	H_2, variety of hydrocarbon fuels (no S)	45 - 60	10-May
SOFC	Oxygen-ion conductor	700 - 1,000	Sr-doped $LaMnO_3$	Ni- or Co-doped YSZ cermet	Impure H_2, variety of hydro-carbon fuels	45 - 55	5-Jan

[a]PAFC, phosphoric acid fuel cell; AFC, alkaline fuel cell; PEMFC, proton-exchange membrane fuel cell (also termed a polymer electrolyte fuel cell, and sometimes a solid pol-ymer electrolyte fuel cell, SPEFC); DMFC, direct methanol fuel cell; MCFC, molten car-bonate fuel cell; SOFC, solid oxide fuel cell.

[b]Reported values of the efficiency of a given type of fuel cell change widely and often no information is provided on the use of the HHV or LHV value. Note that the absolute numbers, the higher heating value (HHV) and the lower heating value (LHV) for hydrogen are 142 and 129 MJ Kg^{-1}, respectively, i.e., the HHV is 18% greater than the LHV. The val-ues that are taken here from the literature should be treated with caution to their exact meaning and are simply included to provide an approximate comparison of the perfor-mance of the respective systems.

[c]Proton-conducting polymer: perfluoro-sulfonic acid polymer.

a) LT (50-150 ºC): alkaline (AFC), proton-exchange membrane (PEMFC), and direct methanol (DMFC) fuel cells [15].

b) MT (medium temperature, around 200 ºC): Phosphoric Acid Fuel Cell (PAFC).

c) HT (600-1,000 ºC): Molten Carbonate (MCFC) and Solid Oxide (SOFC) fuel cells.

Fuel cells are of increasing interest as stationary power sources for the distributed generation of electricity and as portable or mobile power sources for applications ranging from advanced cellular phones to electric vehicles. Currently, their development occurs essentially in the fields of electric vehicles (BEVs) and HEVs. This is due to their potential impact on the environment, e.g., the control of emission of greenhouse gases (GHG). Most major motor companies work solely on PEMFCs due to their high-power density and excellent dynamic characteristics as compared with other types of fuel cells. Fuel cell vehicles (FCVs) have been developed and demonstrated, e.g., GM Hydrogen 1, Ford Demo IIa (Focus), Daimler-Chrysler Ne Car 4a, Honda FCX-V3, Toyota FCHV, Nissan XTERRA FCV, VW Bora HyMotion, and Hyundai Santa Fe FCV. PEMFCs provide continuous power as long as hydrogen fuel is available, and they can be fabricated in small sizes without efficiency loss. Major electronics companies, such as Toshiba, Sony, Motorola, LG, and Samsung, have in-house R&D units for portable fuel cells. The lifetime required by a commercial fuel cell is over 5,000 operating hours for light-weight vehicles and over 40,000 hours for stationary power generation with less than a 10% performance decay [16] in general, a great number of fuel cells exhibit major performance decay after 1,000 hours of operation [17]. Breakthroughs in material development, acquisition of fundamental knowledge, and development of analytical models and experimental tools are particularly important for current fuel cell development.

FCVs face particular problems concerned with the requirement for compactness; the availability and supply of suitable fuel; intermittent operation; the fast start-up from cold; and the high cost. It is generally agreed that hydrogen is the ideal fuel for a fuel cell, but practical methods for its production and distribution and the storage on-board the vehicles in a compact and economic form have still to be devised. Storage schemes under consideration include compressed gas, liquid hydrogen, metal/chemical hydrides, and carbon nanostructures.

Most of the major automotive companies that are investigating FCVs have opted for the solid polymer electrolyte fuel cell that uses an acid membrane that is conductive to hydrogen gas, the so-called Proton Exchange Membrane Fuel Cell (PEMFC). Many different prototype vehicles have been built and demonstrated. Most US companies have used the Ballard fuel cell, manufactured in Canada, which was also exploited by Ford and Daimler Chrysler. General Motors, Honda, Toyota, Nissan, Mercedes Benz, Volkswagen, Volvo, and other companies (e.g., BAE Systems, H2 Logic, Hyundai-Kia, Nuvera, Oorja Protonics, Proton Motor, Hydrogenics, Protonex, Tropical S.A. and UTC Power) have developed their own PEMFC stacks and have tested them in various car models. These PEMFCs have been applied in light-weight vehicles, buses, electric-powered bicycles, forklifts, and auxiliary power units including leisure, trucking, marine, and Unmanned Aerial Vehicles. Distributed PEMFC systems are also being employed in several areas such as heat-power co-generation for household /residential use and uninterruptable power supply. Major companies in these stationary sectors are Altergy, Clear Edge, Ebara Ballard, Eneos Celltech, Hydrogenics, Idatech, Matsushita, P21, Plug Power, and Toshiba FCP.

In the sectors of portable power generation, PEMFCs are being used for mobile phones, laptops, radio control cars, boats, robot toys, emergency lights, and military applications. Major companies in these portable sectors are CMR fuel cells, Viaspace/direct methanol fuel cell corporation, Jadoo power systems, Horizon, MTI micro, Neah power systems, Samsung DSI, SFC Smart Fuel Cell, Sony, and Toshiba. Some small specialist companies like Zevco, Electric Fuel Ltd., eVionyx Corporation, Metallic Power Inc., and Electric Fuel Ltd., have opted for different types of fuel cells, based on alkaline fuel cells, zinc-air fuel cells, and others. The power of electric passenger automobiles, utility vehicles, and bus changed from 20 kW to 250 kW. The stationary power by general fuel cells has a wide range, 1-50 MW. The portable power is usually in the range of 5 - 50

W. At present most car companies are all focused on the development of PEMFC stacks. With large engineering teams devoted to the FCV project and with encouragement from national governments, it would be precipitous to deny the possibility of success.

In this article, we review the fundamentals of PEMFCs, pointing out the advantages and difficulties encountered in their development and application in the transport sector. In particular, we consider the main technical issues of the PEMFCs, e.g., the modelling of electrocatalysts and support materials for the Hydrogen Oxidation Reaction (HOR) at the anode, and the Oxygen Reduction Reaction (ORR) at the cathode, including their activity and stability, thin Bipolar Plates (BPPs) and cooling plates, water removal capacity, gas Diffusion Layers (GDLs) and seals, cost breakdown of the fuel cell stack, durability improvement, operation temperature increase to 120 ºC, and cost reduction. Then, in the second part, we emphasize membrane electrolytes with several desired properties (high conductivity, low swelling, low gas permeability, stability, low cost), to be optimized for use in PEMFCs. The membrane water transport and its mechanisms, as well as the electro-osmotic drag, are also briefly reported, as well as the recent developments based on cation- and anion-exchange membranes for their use in PEMFCs able to utilize a full range of low to high pH environments. More correctly, in the case of anionic conducting membranes being used in hydrogen-oxygen fuel cells, we are no longer dealing with PEMFCs, but with AEMFCs, as reported above.

Proton Exchange Membrane Fuel Cell

The central component of a PEMFC is the so-called "Membrane Electrode Assembly" (MEA), in which a sulfonated polymer membrane (usually, Nafion™ from Dupont Corporation) is sandwiched between the negative and the positive plates. Both types of plates are made from carbon cloth (or carbon paper) with very finely divided platinum as the electrocatalyst. As well as providing the basic mechanical structure for the electrode, the carbon substrate diffuses gas onto the catalyst and therefore is often called the "Gas Diffusion Layer" (GDL).

The configuration of a single cell, together with its electrochemistry, is illustrated schematically in (Figure 2). Outside the MEA are flow-field plates. These contain channels to ensure that each gas is in contact with the whole surface of the respective electrode. They also serve to remove unused gas and the water that is produced at the positive electrode. Sulfonic acid groups ($-SO_3H$) are attached to the carbon chain of the polymer and allow protons to pass through the material. To give maximum conductivity, the membrane must be humidified during operation but must remain sufficiently dry around the electrodes so that the transport of gas is not limited.

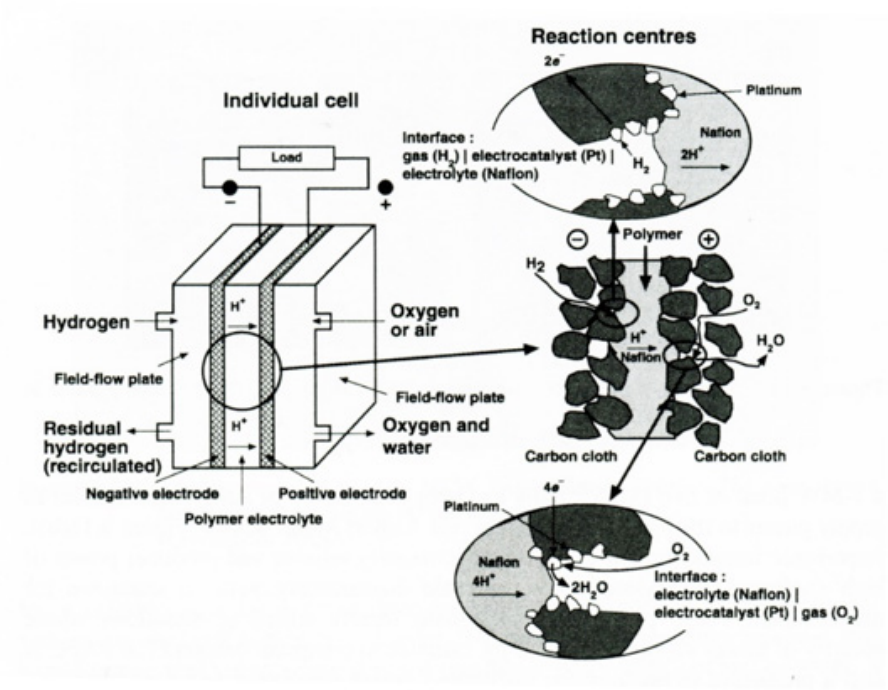

Figure 2: Configuration and electrochemical processes taking place in a PEMFC.

Clearly, for the PEMFC to function properly, flooding of the electrodes by exhaust water must be avoided through careful management. The platinum catalyst is deposited on the surface of the carbon electrodes that are then hot-pressed to the polymer membrane so that the membrane extends partially into the porous electrodes. A gas-electrocatalyst-electrolyte interface (the so-called "three-phase boundary") is formed, such that the electrocatalyst has simultaneous contact with the hydrogen or oxygen/air, the

proton conductor (the electrolyte membrane), and the electron conductor (carbon electrode). The electrochemical reactions occur at these points of simultaneous contact. Below we discuss the two half-cell reactions and the overall reaction when using pure H_2 as fuel, and O_2 as an oxidant, in an acid electrolyte. Hydrogen enters the pores of the anode and reaches the reaction zone, where gas, electrolyte, and the solid conducting structure meet. The hydrogen gas diffuses to the electrochemically active site (e.g., a surface coated with a platinum catalyst), where it is adsorbed and dissolved by the electrolyte. It then dissociates and ionizes to $2H^+$. The protons go through the membrane and electrons run through the external circuit. This reaction, eq.1, is called the HOR [18]. At the cathode, the supplied oxygen combines with electrons from the cathode and hydrogen ions from the electrolyte to produce water, eq.2. This is the ORR forming water as the only product [19]. If the total reaction, eq.3, is related to one oxygen molecule, the process produces a total of four electrons.

$$2H_2 \rightarrow 4H^+ + 4e^- \quad (1)$$

$$O_2 + 4H^+ + 4e^- \rightarrow 2H_2O \quad (2)$$

$$2H_2 + O_2 \rightarrow 2H_2O \quad (3)$$

The water does not dissolve in the electrolyte and is, instead, expelled from the back of the cathode into the oxidant gas stream. As the PEMFC operates at about 80 C, the water is produced as liquid and is carried out of the fuel cell by excess oxidant flow.

The theoretical cell voltage of a fuel cell, not connected to the electrical circuit, at a given pressure and temperature, is given by the Nernst equation. But when the circuit is closed, various voltage losses are caused due to different phenomena. Such losses are broadly classified as charge transfer losses, ohmic losses, and concentration losses. The thermodynamic potential gives the maximum possible voltage from a single cell. The Gibbs free energy is a measure of the chemical potential energy in the reactant and thus, is a measure of the maximum work which can be derived from the chemical reaction. For a reversible electrochemical reaction, the maximum electrical output would be equal to the change in Gibbs free energy. Hence, from the amount of electrical work produced we can obtain the maximum reversible output voltage calculated from equation 4, the thermodynamic Open Circuit Voltage (OCV) of a galvanic cell.

$$E^\circ(T) = -\frac{\Delta G(T)}{zF} \quad (4)$$

E° is the standard potential, ΔG (T) is the change in Gibbs free energy for the reaction which depends on the temperature, z is the number of electrons involved in the reaction and F is Faraday's constant. For the overall reaction in eq. 3, the potential at 25 ºC is 1.229 V. When drawing a current from the cell several loss mechanisms play a role and have to be considered, as described above. Charge transfer polarization is the voltage overpotential required to overcome the activation energy of the electrochemical reaction on the catalytic surface. This type of overpotential dominates at lower current density only. The total charge transfer overpotential is 0.1-0.2 V, which reduces the maximum actual voltage to less than 1.0 V even under open-circuit conditions. The material`s natural resistance to charge flow causes ohmic resistance, which results in a loss in cell voltage.

This resistance is offered by all the components of a fuel cell, e.g., the carbon electrodes, current collecting plates, and contact material to the circulation of electrons, and the resistance of the electrolyte membrane to transfer the protons through it. The specific resistance of the membrane is dependent on the water content of the membrane which itself is affected by the relative humidity/water content of the incoming gas streams and thus the dry gas and dew point temperature. The concentration losses arise because of the inability of the cell to deliver the required amount of oxygen at constant pressure due to flow resistance. As the reaction proceeds and current density increases, the concentration of reactant increases, and thus, its concentration at the electrode surface decreases while the rate of diffusion of gas through the Gas Diffusion Layer (GDL) is comparatively low because of a number of factors. Such a phenomenon will put an upper limit on the rate of reactant consumption. Equation 5 summarises the main factors contributing to energy loss.

$$E_{cell}(I,T) = E_{rev}(T) - i.R_{ohmic}(i,T) - \eta_{ORR}(i,T) - \eta t(i,T) \quad (5)$$

Here I denotes the current density of the cell, with R_{Ohmic} (i, T) describing the ohmic resistance of the cell as a function of current density and temperature. The loss at the cathode from mass transport and at the anode are denoted η_{ORR} (i, T) and η_t (i, T) respectively, and are also functions of current density and temperature.

Erev (T) is the reversible potential of the fuel cell, considering the partial pressures of reactants and products. It is calculated using the Nernst eq. 6, where R is the gas constant and Px is the partial pressure of the reactants and products. Losses from the anode have been neglected as they are small in comparison to the rest when utilizing Pt as HOR catalyst. Thus, it is clear that the main losses in the fuel cell can be attributed to the ORR and in turn the slow kinetics of this reaction.

$$E_{rev} = -\frac{\Delta G(T)}{zF} + \frac{RT}{zF}\ln\left(\frac{PH_2\sqrt{PO_2}}{PH_2O}\right) \quad (6)$$

For automotive usage, the PEMFC class holds many advantages that make it the technology of choice. It has an operating temperature range overlapping with that of Internal Combustion Engines (ICEs), high conductivity of the membrane as well as an overall high electrical efficiency.

The voltage of a PEMFC lies in the range of 0.8 - 0.6 V, as determined by the current density. If it is assumed (generously) that the average voltage is 0.75 V, then the fuel cell is 50% efficient, i.e., half of the energy content of the hydrogen is converted to low-voltage d.c. electricity. In addition, allowances have to be made for parasitic currents and self-discharging, parallel electrochemical reactions yielding fewer electrons per mole of reactant consumed, chemical reactions of reactants catalysed by the electrodes, a direct chemical reaction of the two electrode reactions, pumping of the fuel and the oxidation material, and also the necessary energy for heating, cooling, electrolyte pipes, compression, and auxiliary installations, the cell design, and the vehicle's electrical system. In round figures, the collective losses in each system can be taken as 10%. Thus, the overall efficiency of converting hydrogen to traction effort is 0.5 × 0.9 × 0.9 = 40%. Although this is much higher than for a high-performance automobile (20-25%), as emphasized by advocates of FCVs, the losses incurred in producing hydrogen from primary fuels must also be considered.

The steam reforming of natural gas to hydrogen on a large scale is 60 - 70% efficient. It is next reasonable to assume at least a further 10% energy loss in compressing the hydrogen and 10% in transporting it from the centralized steam reformer to the vehicle-refueling depot. The overall efficiency from natural gas to traction effort, via hydrogen, is then around 0.65 × 0.9 × 0.9 × 0.4 = 21%. In other words, FCVs have a performance that is very similar to that of today's petrol engines-they would, however, help to reduce urban pollution from road transportation.

What if the hydrogen is produced by electrolysis rather than directly from natural gas? Here the situation is even direr. For a conventional power station, the efficiency is about 30% (coal-or nuclear-fire) to 55% (combined-cycle gas turbine). The best electrolysis is around 80% efficient. The overall efficiency from primary fuel to traction effort is then:

$$\text{coal or nuclear: } 0.3\times 0.8\times 0.9\times 0.9\times 0.4 = 8\%$$

$$\text{natural gas: } 0.55\times 0.8\times 0.9\times 0.9\times 0.4 = 14\% \quad (7)$$

Here the loss in compressing the hydrogen has been retained and the loss in distributing hydrogen has been replaced with a 10% loss in the electricity-supply system. The above analysis clearly shows that there is no incentive to move from the internal-combustion engines to the fuel-cell vehicle. The large availability of renewable electricity determined by reduced costs, political acceptability, and the existence of a practical means of electricity storage within the grid system, should improve the overall efficiency figures as shown above. This is because the conversion of mechanical energy to electrical energy does not involve a Carnot cycle and the efficiency should be 80 - 90% rather than 30-55%. In the meantime, it should be noted that the efficiency of internal-combustion engines is expected to improve rapidly, as demonstrated by recent projections for various configurations of family-sized cars. Thus, by converting to hybrid vehicles-a perfectly feasible proposition by 2025/2030-it should be possible to reduce fuel consumption by two-thirds compared with the nineties model family car. This seems a much more realistic option than that of fuel-cell cars, on both energy efficiency and cost grounds.

The use of platinum is a major factor in PEMFC cost and research in the nineties was directed at reducing the size of the particles and spreading them more evenly. Pt was necessary because the environment in a PEMFC is very corrosive due to the acidic nature of the proton exchange membrane and the working potential that promotes the dissolution of most metals [20]. Modern cells can op-

erate with a total electrocatalyst loading (both electrodes) of 0.2 mg cm^{-2} (0.5 g per kW peak). It should also be noted that, because of the lower operating temperature of the PEMFC, the platinum electrocatalyst is more susceptible to poisoning by carbon monoxide than that used in a PAFC. Accordingly, the carbon monoxide level must be kept below 5 ppm. This archetypal reversible PEMFC impurity is present whenever methane is reformed into hydrogen or when other impurities (e.g. carbon dioxide and formic acid) are present at the anode [21]. There is also work in progress to develop new membranes that will enable fuel-cell operation at higher temperatures. This would yield significant energy benefits. For example, heat rejection would be easier and would allow using smaller heat exchangers in fuel-cell systems. In addition, with reformate systems, tolerance of the stack to carbon monoxide is less problematic at high temperatures.

With the launch of the Toyota Mirai a new catalyst has seen commercial use; an improved Pt-Co alloy, with close to double the activity per gram of Pt, that in part has made it possible to actually increase enormously the fuel cell market [22-24]. With Pt as the catalyst, the amount needed for a single FCEV with 100 kW output would have been around 50 g of Pt. The price for a single car at this usage would be roughly 1,600 $ per-car in raw metal price, without processing. The production of 500,000 FCEVs would use a quarter of all the Pt used for catalytic converters. That might seem acceptable, however, car production totals over 70 million cars per year. As with other FC designs, single PEM cells can be stacked together, in series electrically, to form a module with higher voltage. A schematic of a typical configuration for a two-cell module is given in (Figure 3). The individual MEAs are separated by BPPs, which are usually 3 mm or less in thickness, and are made from graphite foil or graphite polymer composites [25].

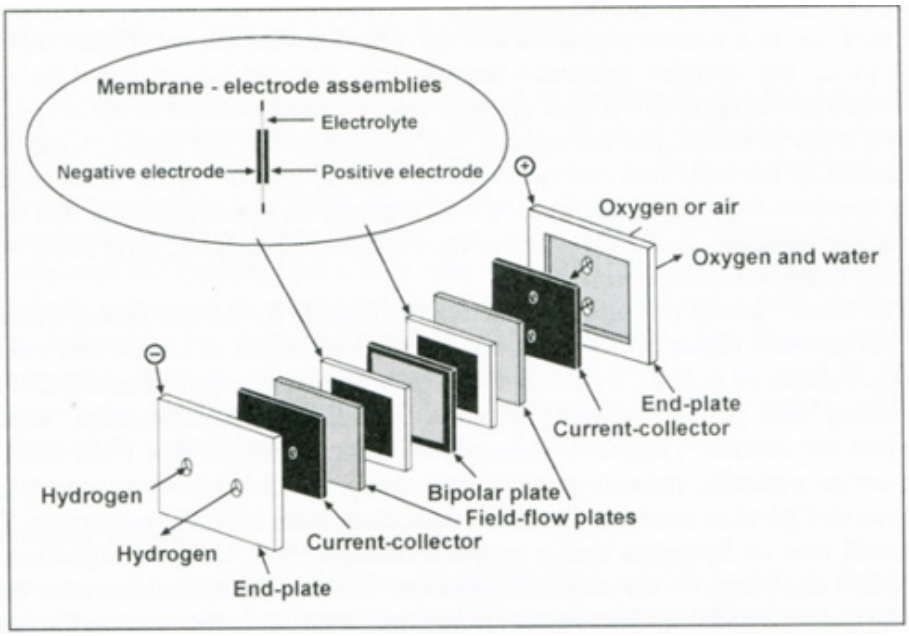

Figure 3: Structure of two-cell PEMFC module.

Each bipolar plate is in contact with the negative electrode of one MEA and the positive electrode of the next, i.e., in a manner similar to that of a bipolar electrolyzer (Figure 4). The plates are complex structures because they have to supply the cells with hydrogen and oxygen/air (on their opposite sides), conduct current to the next cells, enable water to escape, prevent leakage of gases, and collect and remove the waste heat produced by the cell. Fuel cell stacks using such designs of BPPs require only two flow-field plates, one at each end. It should be noted, however, that there are minor variations in stack design between different developers, particularly for the sub-components. The Nexa™ power module, manufactured in Canada by Ballard Power Systems Inc., is shown in (Figure 5). This unit has a power output of 1.2 kW and weighs 13 kg. Introduced in 2001, it became the world's first volume-produced PEMFC for stationary and portable power-generation applications. A subsequent Ballard product, the AirGen™, has been designed for indoor operation. This 1-kW PEMFC can act as a standby uninterruptible power supply and has a built-in suppression system that protects sensitive electronic equipment from high-voltage surges. The fuel-cell runs on hydrogen that is supplied through either industrial cylinders or canisters according to the required operation time. Field trials have also been conducted on 250-kW PEMFC plants to evaluate their suitability and performance as distributed power generators for commercial and residential consumers.

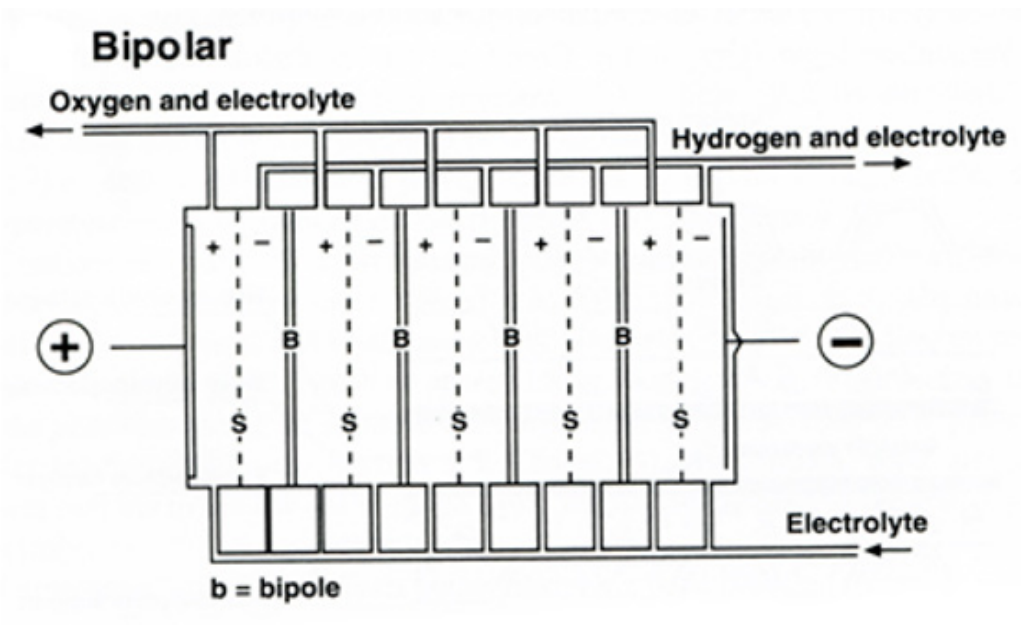

Figure 4: General arrangement of bipolar - electrolyzer modules.

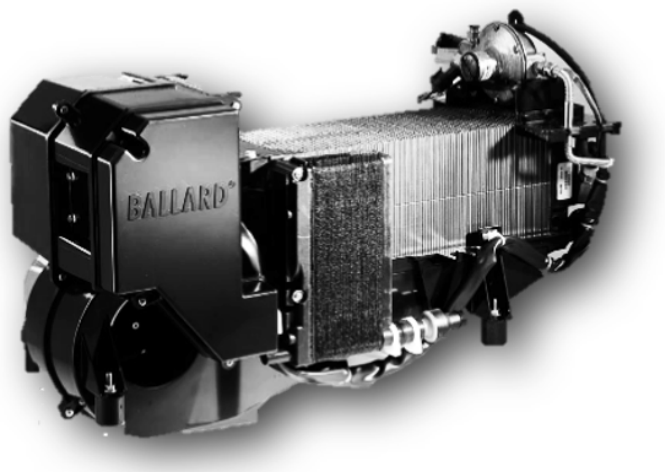

Figure 5: Portable Nexa™ power module.

Hyundai Motor announced the Tucson motorcar, having zero-emission for the ultimate drive of 400 km, on one tank of fuel. Honda motor Company's fuel cell car, Clarity can be filled up in a few minutes and travel up to 366 miles on a tank. There are also several reports on producing fuel cell engines and their use in Yamaha FC-me fuel cell motorcycles, Mercedes-Benz Citaro fuel cell buses, hydrogen fuel cell boats, and even trains like the Coradia iLint full emission-free regional train. The Boeing Company demonstrated a lightweight airplane that can fly having a fuel cell engine as its power source. Despite the high cost of fuel, technology, and the low durability of catalysts [26-31], manufacturers have devoted much effort to solving many fundamental issues and difficulties in the production of large amounts of fuel vehicles. To reduce the timeline of fuel cell development toward commercialization, it is necessary to surpass the following shortcomings:

a) The electrodes are at present the costliest components, provided the fuel cells are made in large quantities. As the platinum content of the electrodes is the cost-determining factor, and being a noble metal, its cost will not decrease with increasing quantity. The most advanced alternative alloy catalysts for replacing platinum at the electrodes can be classified as Pt-based electrocatalysts [32,33], non-platinum precious-metal-based electrocatalysts [30,34-36], non-precious metal electrocatalysts [37-40], and carbon-based metal-free electrocatalysts [41-43]. Highly active catalysts having an abundant number of active sites, with stable structure, durability, and reduced cost, are urgently needed. In this context, the US Department

of Energy set a 2025 durability target of 8,000 h (equivalent to 150,000 miles of driving) with less than 10% of performance loss, to compete with automotive internal combustion engines.

b) Currently, Pt or Pt-based materials are still the most commonly used catalysts that exhibit state-of-the-art performance for the PEMFC, namely for its ORR. The urgent need to reduce the PGM catalyst loading is pushing the introduction and further development of metal and non-metal-supported electrocatalysts, particularly if they meet some general requirements, for example, high surface area, high electronic conductivity, stability under an acidic environment, uniform dispersion of noble metal nanoparticles on it, effective metal-support interaction, porous structure for reactant gas access to the electrocatalysts, and low-cost. The catalyst support plays a vital role in deciding the overall MEA performance because it participates in the construction of a three-phase boundary (TPB) for charge and mass transport. Carbon blacks, as the widely used support materials for fuel cell catalysts, include XC-72 and Ketjen black, etc., which are adopted due to their high conductivity, low cost, and great performance. However, the corrosion of carbon black supports at high potential significantly degrades the catalyst performance via migration and agglomeration, along with the detachment of surface-loaded Pt nanoparticles. This carbon corrosion is most commonly caused by the formation of a hydrogen-air interface in the start-up/shutdown stage of the vehicle operation. Carbon substrate corrosion will decrease the Brunauer-Emmett-Teller (BET) surface area of Pt and increase the number of oxygen-containing groups on the carbon surface, causing facile dissolution and Ostwald ripening of Pt nanoparticles, and weakening the Pt-support interaction, which triggers detachment and agglomeration of Pt nanoparticles. As carbon with a low degree of graphitization is prone to corrosion, ideal carbon supports should have sufficient long-range ordered graphitic structures, and favourable surface properties to reinforce metal-surface interactions and disperse nanoparticles uniformly. The direct indicator of the stability of carbon support is its weight loss or CO/CO_2 emissions during cycling. Therefore, enhancing the antioxidation capacity of carbon supports and rapidly evaluating their electrochemical stability can effectively speed up the development of highly durable catalysts for automotive PEMFCs. An ideal support should also offer a mesoporous structure enabling the ionomer and polymer electrolyte to bring the electrocatalyst nanoparticles close to the reactants, and good water handling capability to avoid flooding. Hence, a good support material is vital in determining the behaviour, performance, durability, and cost-effectiveness of the catalyst and the overall fuel cell. A multitude of materials have been investigated as catalyst supports for PEMFCs, namely nanostructured carbon supports (carbon nanotubes, carbon nano-fibre, mesoporous carbon, nanodiamonds and doped diamonds, graphene), non-carbonaceous and inorganic oxide/carbide supports (titanium oxides, titanium nitride, titanium diboride, other dopants for titania, tin oxide, indium tin oxide, silicon dioxide, tungsten oxide, tungsten carbide, sulfated zirconia), conducting polymers and hybrid supports [44,45]. An amalgamation of these novel electrocatalyst supports and improved catalyst loading techniques could bring about revolutionary changes in the quest for high-performance, long-lasting PEMFCs.

c) BPPs [25,46-48] are one of the key components of a fuel cell that comprises around 75% of its weight and 45% of its price; they undertake the crucial functions of distributing reactant gases and cooling medium, collecting the electricity generated, exporting waste products, etc. Various methods have been proposed to fabricate metallic BPPs [49-53] such as stamping which presents a high potential for mass production. Since a BPPs works in an acidic environment, it should have excellent corrosion resistance, and avoid toxic ion emission during fabrication. As a result, titanium raises as a proper option due to its excellent corrosion resistance and low density. But cheaper materials such as stainless steel are also promising and can provide satisfactory performance for several thousand hours. Other materials are polymeric such as polypropylene and polymer/graphite compounds. Note that the flow field on the bipolar plate [53] needs to be carefully designed to minimize the concentration overpotential with high electrical conductivity and strong mechanical properties. Due to unique advantages such as being ultra-thin, high strength, easy-to-mass-produce, etc., metallic BPPs have been considered as the promising solution for automotive and aerospace application scenarios with a strong requirement of power density.

d) Gas diffusion layer (GDL) [54] is one of the critical components of a fuel cell that has the ability to influence the H2/air system as its basic functions are the transportation of the reactant gas from flow channels to Catalyst Layer (CL) effectively, draining out liquid water from CL to flow channels, conducting electrons with low resistance and keeping the membrane in wet condition at low humidity. The GDL should possess the combined and balanced properties of hydrophobicity (water expelling) and hydrophilicity (water retaining). These properties have to be balanced carefully to ensure that the fuel cell system works without flooding and high humidity. The ideal GDLs should have properties such as good gas diffusion, with optimum bending stiffness, porosity, surface contact angle, air permeability, water vapour diffusion, electrical/electronic conductivity, crack-free surface morphology, high mechanical integrity, and enhanced oxidative stability along with durability at various operating conditions including freezing. The GDL has a complex pore structure, and its transmission characteristics have an important influence on the performance of PEMFC, particularly in questions such as mass transport, permeability, and tortuosity. Conducted experimental studies on these effects are time- and effort- consuming. Accordingly, groups of image combination techniques and stochastic techniques, are being adopted recently.

e) The membrane [55-57] refers to a thin layer of electrolyte, which conducts protons from the anode to the cathode. Desirable membrane materials are those that exhibit high ionic conductivity while preventing electron transport and the crossover of hydrogen fuel from the anode and oxygen reactant from the cathode. In addition, they must be chemically stable in an environment with OH- and HOO radicals, thermally stable throughout the operating temperatures, and mechanically robust. Current membranes are mostly based on perfluorosulfonic acid, the most prominent of which, Nafion, was first developed by the Dupont Company in the 1960s. Nafion has a structure of copolymer from fluoro3, 6-dioxo 4,6-octane sulfonic acid with poly-tetra-fluorethylene (PTFE). The ionic group of the structure has a very high water-of-hydration, so the Nafion polymer very efficiently absorbs water. This hydrated polymer allows very rapid transport of water and its protons, as well as of dried and humidified gases and other species, namely organic residues, which is essentially due to the interconnections between the sulfonic acid groups. But the chemical nature of the polymer itself is not changed by this process; in other words, its properties of water permeability, ion-exchange, and acid catalysis are not directly affected. There is significant interaction between the desired properties of the membrane - high conductivity, low swelling, low gas, and methanol permeability, and stability -and the type of backbone polymer, the degree of sulphonation, and the nano-phase separation into hydrophilic and hydrophobic domains. To satisfy these requirements, different approaches have been examined: sulphonated perfluorinated materials with and without microporous support; sulphonated polyhydrocarbons; acid-base complexes and blends with a surplus of acid ionic groups; and inorganic-organic composite materials with improved thermal stability and better water-retaining properties. The most important property of the membrane is proton conductivity which relates to the extent of the humidity of the membrane. A higher extent of humidity allows higher proton conductivity. The Equivalent Weight (EW) and membrane thickness are also key properties of the membrane. Decreasing the EW (which is defined as grams of dry polymer per mole of the acid group) can increase the proton conductivity of the membrane; however, the mechanical strength will decrease. Deducing the thickness of the membrane can significantly improve the performance because the thinner membrane leads to lower membrane resistance and lower cost of the materials. However, a thinner membrane will bring durability and hydrogen by-pass issues. To achieve an applicable membrane, one always needs to balance membrane thickness and proton conductivity. It should be emphasized that if an alternative membrane material does emerge, considerable R&D will still be necessary to optimize and manufacture the new membrane-electrolyte assembly (MEA). This development has taken many years for Nafion-type MEAs, although some of the expertise gained may be able to be transferred to the new system.

f) Clean, energy-efficient PEMFCs are appealing power sources for cars, as well as stationary and portable power sources. Furthermore, their integration into microgrids has been gaining traction around the world, encouraging the usage of hydrogen energy. However, besides cost reduction, durability is the most important issue to be solved before the commercialization of PEMFCs can be successful. To ensure high efficiency and longevity several lifetime goals must be met related to conditions such as fast cycling, repetitive stops and starts, freezing/thawing, new decay mechanisms, anode/cathode contamination by C, S, O, N, H impurities, ECSA reduction, low humidification, higher temperatures, and fuel starvation. For membranes, the most detrimental conditions are reduced cell humidity, especially in combination with open circuit voltage and an increase in temperature. After elucidating the cause of membrane degradation (lower chemical resistance), efforts at the membrane manufacturers have been focused on lowering the density of end-groups (e.g. sulfonic acid groups and other side chain length groups existing in Nafion, Dow, Aciplex, and other proton exchange membranes), which has led to a new generation of membranes, as reported in this article, which has an order of magnitude better resistance (higher chemical stability) towards such membrane degradation conditions compared to the previous generation. In fact, studies of the dynamics of hydronium acids and water molecules have shown that the end-groups density alters actively the overall hydronium/water mobility, leading to a better resistance of the polymer (i.e., better chemical stability), although there is a decrease of proton conductivity (i.e., higher ionic resistivity). These so-called chemically stabilized membranes are widely available, and the problem could be regarded as practically solved. The situation for electrode stability is less positive. Over the life of a fuel cell in a passenger vehicle, a fuel cell will be exposed to an estimated 17,000 start/stop cycles, 1,650 freeze/thaw cycles, and 1,200,000 load cycles [58]. Voltage cycling (which automatically results from load cycling when no capacity between cycling in power demand and the fuel cell is placed) leads primarily to platinum dissolution and particle growth at the cathode. The resulting loss in platinum's surface area leads either to voltage loss and thus to loss in fuel cell efficiency at constant power, or to loss of power at constant cell voltage. Start-stop cycles can lead to extremely high cathode potentials, as high as 1.4 V, which especially leads to corrosion of the carbon support. Besides having a direct impact on the electrode's electronic conductivity, it is the most abundant component in the electrode structure, so its corrosion has a detrimental effect on the integrity of the electrode. The most detrimental condition during start/stop cycles has been pinpointed as the occurrence of hydrogen/air fronts on the anode side. This knowledge can be used to minimize the residence time of such fronts by properly flushing the anode chamber during start-up and shut down. In summary, the PEMFC has advanced to a state that it can successfully be applied in transport applications with specifica-

tions that meet customer expectations.

With respect to activity, stability, durability, material criticality, supply risk, hydrogen impurities, operating temperature, humidified conditions, degradation, cost, and other issues which can lead to irreversible loss in performance, we have seen that many measures have been developed to prevent such performance loss.

The status of PEMFC technology development and application particularly in the transportation sector has been presented above. An important topic that needs to be addressed with greater detail concerns the membrane electrolytes, which will be described in section 3. But before concluding the present section, it seems appropriate to pursue our analysis of the fuel cell system, by deeper considerations of the phenomena involved in PEMFC operation and its complexity. These phenomena and their fundamental issues that are key to fuel cell design, operational control, and material development, involve heat transfer, species and charge transport, multiphase flows, electrochemical reactions, water and thermal management, dynamic operation, cold start, operating pressure, stoichiometric ratio, coolant temperature, mixing of contaminant gases, channel two-phase flow, and low humidity operation. These multi-physics phenomena, very important to overcome the durability and cost barriers, occur in various components of the operational fuel cell, namely, the MEA consisting of CLs and membrane, GDLs and Micro-Porous Layers (MPLs), Gas-Flow Channels (GFCs), BPPs, anode parallel flow field, and cathode serpentine flow field. In general, the anode and cathode flows are in opposite directions, i.e., there is a counterflow arrangement.

To further realize the multi physics above, here are detailed avenues that take place during fuel cell operation:

a) hydrogen gas and air or oxygen is supplied to the electrodes (which must be porous to allow the gas in), by pumping them through the GFCs, respectively.

b) the gases are preventing of leaking in or out through the edges of the porous electrodes.

c) the gases flow through the respective porous GDLs/MPLs and diffuse into the respective CLs.

d) at the anode CL the hydrogen gas ionizes, releasing electrons and creating H+ ions or protons; this reaction releases energy.

e) protons migrate and water is transported through the membrane electrolyte.

f) electrons produced at the anode pass through an electric circuit to the cathode.

g) at the cathode CL oxygen reacts with electrons taken from the electrode, and H+ ions from the electrolyte, to form water.

h) the water formed at the cathode would keep the electrolyte at the correct level of hydration; at the same time, air would be blown over the cathode, and apart from supplying the necessary oxygen it would dry out any excess water; moreover, because the membrane electrolyte is so thin, water would diffuse from the cathode side to the anode, and throughout the whole electrolyte a suitable state of hydration would be achieved, without any special difficulty; this is a happy situation, but complications such as the electro-osmotic drag (typically between one and five water molecules are dragged for each proton during its movement from the anode to the cathode), and the fact that at temperatures over 60 C, the air will always dry out the electrodes faster than the water that is produced by the hydrogen/oxygen reactions.

i) heat is generated due to inefficiencies, mainly in the cathode CL due to sluggish ORR, and is conducted out of the cell via carbon support and BPPs.

j) the transport phenomena are three-dimensional because the flows of fuel (H_2) and oxidant (O_2) in the anode and cathode GFCs are usually normal to proton transport though the membrane and gas transport through the respective GDLs/MPLs and CLs. Fundamental models have been developed to examine the transport processes; the governing equations are the continuity equation, the momentum conservation, the energy conservation, the species conservation (water/hydrogen/oxygen), the electrons charge conservation, and the protons charge conservation [59-65]. (Table 2) lists the typical ranges of most model parameters.

Table 2: Frequent Electrochemical and Transport Properties.

Description	Unit	Value
Electrochemical Kinetics		
Exchange current density (Anode, Cathode), i_0	A m^{-3}	10^9, 10^3 - 10^4
Faraday constant, F	C mol^{-1}	96487
Electrical conductivity of DMs, BPs, σ^{eff}	S m^{-1}	300, 20000
Species Transport Properties		
H_2/H_2O diffusivity (H_2-H_2O) at standard condition, D^k	m^2 s^{-1}	8.67/8.67 × 10^{-5}
O_2/H_2O (v) diffusivity in the ar at standard condition, D^k	m^2 s^{-1}	1.53/1.79 × 10^{-5}
Viscosity at 80 ºC (H_2/Air), D^k	m^2 s^{-1}	9.88 × 10^{-6}/1.36 × 10^{-5}

Thermal Properties		
$H_2/N_2/O_2/H_2O$ (v) thermal conductivity, k^{eff}	W m^{-1} K^{-1}	0.170/0.024/0.024/0.024
Anode/cathode GDL conductivity, k^{eff}	W m^{-1} K^{-1}	0.3 - 3.0
Anode/cathode CL conductivity, k^{eff}	W m^{-1} K^{-1}	0.3 - 1.5
Membrane thermal conductivity, k^{eff}	W m^{-1} K^{-1}	0.95
Anode/cathode bipolar plate thermal conductivity, k^{eff}	W m^{-1} K^{-1}	> 10.0
$H_2/N_2/O_2/H_2O$ (v) specific heat at 80 ºC, C_p	J kg^{-1} K^{-1}	14400/1041/917/2000
Anode/cathode GDL heat capacity, ρC_p	J K^{-1} m^{-3}	5.68×10^5
Anode/cathode CL heat capacity, ρC_p	J K^{-1} m^{-3}	1.69×10^6
Membrane heat capacity, ρC_p	J K^{-1} m^{-3}	1.65×10^6
Anode/cathode bipolar plate heat capacity, ρC_p	J K^{-1} m^{-3}	1.57×10^6
Latent heat of liquid water-vapour/liquid-solid water phase change	J kg^{-1}	$2.26 \times 106/3.34 \times 10^5$
Material Properties		
Permeability of anode/cathode GDL, KGDL	m^2	1.0×10^{-12}
Permeability of anode/cathode CL, KCL	m^2	1.0×10^{-13}
Anode/cathode GDL porosity, ε		0.4 - 0.8
Anode/cathode CL porosity, ε		0.3 - 0.5
Ionomer volume fraction in CL, εm		0.13 - 0.4
Equivalent weight of ionomers, EW	kg mol^{-1}	0.9, 1.1, or 1.2*
Dry density of membrane, ρ	kg m^{-3}	$1.98 \times 10^{3*}$

The CL is where the HOR or ORR takes place. CL is usually very thin (about 10μm) [66]. The catalyst, which usually contains several phases (carbon support with Pt catalyst particles dispersed on the carbon surface, ionomer, and void space), plays the critical role of reducing the reaction activation barrier. A recent paper by *Etesami, et al*. [67] focuses on the progress of the research related to the development of electrocatalysts practically used in PEMFCs, where the corner-stone reactions are ORR and HOR. The review, with 176 references, highlights recent electrocatalysts that have been used in PEMFCs, stressing that novel structured electrocatalysts are much required for future electrochemical energy-related devices, as replacements for Pt.

GDLs and MPLs play multiple roles in the fuel cell, as reported in [4,68]. Apart from diffusive transport, physical processes in GDLs include bypass flows induced by an in-plane pressure difference between neighbouring channels [69], through–plane flow induced by mass source/sink due to electrochemical reactions [70], heat transfer [9,15,46], two-phase flow [71], and electron-transport [72]. Gas Flow Channels (GFCs), located within the BPPs [25,46,49] with a typical cross-section dimension of around 1mm, supply gases for reactions and remove by-product water. BPPs provide mechanical support over DMs and conductive passages for both heat and electron transport. BPP degradation [49,52], such as metal plate corrosion and graphite crack, may happen and reduce fuel cell lifetime [15]. Cooling channels are essential for waste heat removal for large-scale fuel cells. Local hot spot formation can degrade the membrane and cause pin-hole or crack formation [73].

The growth and detachment of liquid water droplets at the GDL/GFC interface are influenced by two factors: the operating conditions of the fuel cell and the physical (e.g., surface roughness) and chemical (e.g., wettability) material characteristics of the GDL surface (e.g., in terms of the hydrophilic/hydrophobic properties). *Chen, et al.* [74] pioneered the analysis of droplet instability and detachment, by constructing instability diagrams, and they indicated that the static contact angle and contact angle hysteresis (the difference between advancing and receding contact angles) are both important parameters in determining the force to move a droplet across a surface. Unstable conditions are desirable to operate the fuel cell under such conditions that droplets can be removed instantaneously from the GDL/GFC interface to prevent blockage of pathways for oxygen transport to the three-phase reaction sites.

The voltage of a single fuel cell is low (less than 1 V under load) and therefore many cells are packed together into multicell stacks or batteries, connected in series or parallel according to the voltage or current requirements. The stack construction also depends on the configuration of the system. A sequential stack design out of prefabricated units is, for example, necessary for the circulation of reactants and coolants in an immobile (matrix) electrolyte system and the provision of electrolyte loops in mobile electrolyte systems. At the stack level, water, heat management, electrical connection, and flow field [70], become more complex due to the interaction of constituent individual cells. A fuel cell with high flow resistance can cause local reactant starvation, thus performance decay and material degradation. A fuel cell with a large thermal resistance may also

reduce its performance and raise concerns about materials degradation. Further issues at the stack level requiring fundamental study are: - stack design and reactant manifold, fuel management, reformer, steam generator, shift reactor, power and electric subsystem, cooling, heat exchanger, and ancillary subsystem [75].

Polymer-Based Electrolyte Membranes

Introduction

Among membrane electrolytes, Solid Polymer Electrolyte Membranes (SPEMs) play a vital role in water electrolysis [76,77], and PEMFCs [78-80]. The properties desired for their use as a proton conductor in PEMFCs include mechanical, chemical, and electrochemical stability in the operation conditions of the system, as well as component compatibility with the bonding requirements of the PEMFCs. Also, high proton and electrolyte transport supports high currents with low resistive losses and maintain uniform electrolyte content, preventing localized drying. To maximize coulombic efficiency (i.e., the ratio between the current or charge observed from the fuel cell and the theoretically expected current or charge due to the amount of hydrogen reactant consumed, assuming that the overall reaction in the fuel cell proceeds to completion), low permeability to reactant species is also a desired property. And lastly, competitive costs of production. The lack of some, or several, of these properties, such as high cost or poor performance, lead many research groups to focus on the development of low-cost polymer-based electrolyte membranes for fuel cell applications. On the other hand, SPEMs have received considerable attention over the last 40 years owing to their wide applicability to batteries, sensors, or electrochromic devices [81-85]. Here, we discuss progress on different SPEMs in PEMFCs.

Perfluorinated membranes

Introduced by DuPont in 1966, the Nafion membranes family exemplifies this membrane type. According to the DuPont de Nemours process, classic Nafion membranes undergo a four-step synthesis [86]. The reaction of tetrafluoroethylene with SO_3 to form the sulphone cycle is the first step. The second step is the condensation of these products with sodium carbonate followed by the formation of an insoluble resin by copolymerization with tetrafluoroethylene. The resin is then submitted to a hydrolysis reaction to form a perfluorosulphonic polymer and, in the last step, the chemical exchange of the counter ion Na^+ with the proton in an appropriate electrolyte. These membranes have played a crucial role in advancing electrochemical system applications, meeting the requirements of various systems like chloralkali, fuel cells, and other non-fuel cell applications. In their general formula, depicted in (Figure 6) [87], the values of x, y, and z are x = 6 - 10; y = z = 1, respectively. Variations in these values result in materials with different Equivalent Weights (EWs) and pendant chain lengths.

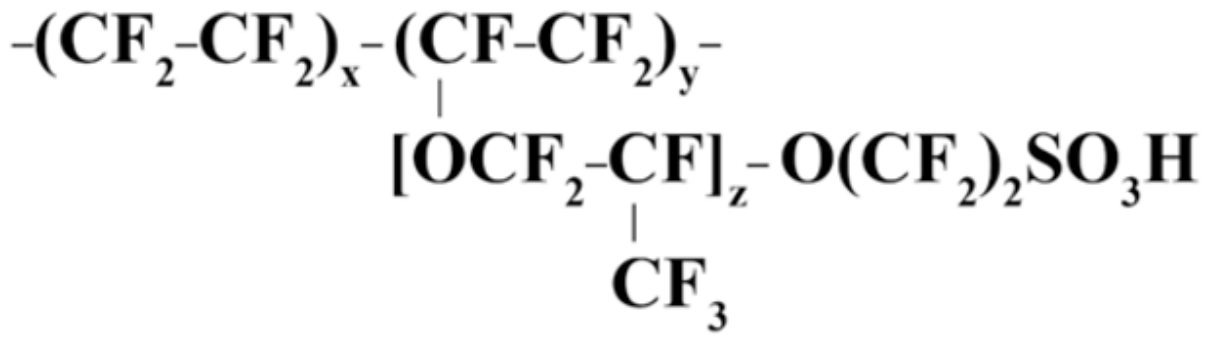

Figure 6: General structure of Nafion membrane: x = 6 - 10 y = z = 1.

The initial high EWs of the Nafion family limited their application in fuel cells, leading to the development of Dow membranes. Structurally similar to Nafion, Dow membranes possess shorter EWs, typically in the 800 to 850 range, and shorter chain lengths [88]. Dow membranes demonstrated significant increases in Solid Polymer Fuel Cell (SPFC) performance during tests conducted in 1987 and 1988 [89]. Addressing limitations with their initial membranes, DuPont further reduced the EW from 1,100 (Nafion 115) to 1,000 (Nafion 105) and the membrane thickness from 7 to 5 mils to enhance power densities. Nafion 115 (5 mils) and Nafion 105 (5 mils) were specifically developed for fuel cell applications. Perfluorinated ionomer membranes have also been developed by the Asahi Chemical and the Asaki Glass Company and commercialized as Aciplex-S and Flemion, respectively. The general properties of the long sidechain perfluorinated ionomer membranes (e.g., Nafion/Flemion/Aciplex) and the short sidechain perfluorinated ionomer membranes (e.g., Dow) are shown in (Table 3). The long sidechain above perfluorinated polymer electrolytes has been proven to have a prolonged service life under electrolysis and electrosynthesis and in fuel cell systems [90].

Table 3: Properties of perfluorinated ionomer membranes.

EW range	800 – 1,500
Conductivity range (S cm^{-1})	0.20 - 0.005
Conductance range (S cm^{-2})	2 - 20
Dimensional stability	10 - 30% expansion X and Y direction from 50% RH liquid water (25 ºC). For example, 100 EW = 16% expansions
Proven lifetime	> 5,000 hours.
Thickness (µm)	50 - 250

They are not efficient for high-temperature (≥ 150 ºC) fuel cell systems because their conductivity decreases significantly due to their dehydration. Although some efficiencies have been gained by lowering the membrane EWs, the main improvement advantages in fuel cell performance were realized by simply thinning the membranes [91]. The advantages gained with this simple strategy include lower membrane resistance, less material utilization (and related cost savings), and improved hydration of the entire membrane. To improve high-temperature performance, studies have been made with ultrathin membranes [92], however, there is a limit to the extent to which such membranes can be thinned because of difficulties with durability and reactant crossover.

Various methods have been employed to modify perfluorinated membranes, such as incorporating hygroscopic inorganic fillers (e.g., silica, ZrO_2, and TiO_2) to enhance proton conductivity via water retention [93-96] and mechanically reinforcing perfluorinated composite membranes with polytetrafluoroethylene (PTFE) backbones [97-105]. Perfluorinated Membranes Reinforced with woven PTFE, such as Nafion 334 or 417, find applications in industrial electrochemical processes. In the 90s, non-woven PTFE/perfluorinated ionomer composite membranes were developed for ion transport studies [106,107] and investigations of other properties relevant to fuel cell applications [108].

Most Ion Exchange Membranes (IEM), including perfluorinated ones, incorporate some form of reinforcement due to their inherent weakness and substantial swelling when exposed to solvents. Reinforcement can be in the form of "macro-reinforcement" or "micro-reinforcement." Incorporating PTFE into perfluorinated ionomer membranes can effectively lower material costs with less perfluorinated ionomer, increase mechanical strength, and maintain comparable fuel cell performance to conventional membranes. A typical approach involves incorporating a perfluorinated ionomer solution into the pores of porous PTFE substrate membranes through methods like direct dip-coating or impregnation. In general, a perfluorinated ionomer solution is incorporated in the pores of porous PTFE substrate membranes by direct dip-coating or impregnation methods. *Jung, et al.* [100], and *Weng, et al* [102] reported on studies with incorporated silicates in the Nafion/PTFE composite membranes, which revealed enhanced water retention at high temperatures and low Relative Humidity (RH). *Yoon, et al.* [104] disclose the development of a reinforced PFSI/PTFE composite membrane by the introduction of polydopamine as an interfacial modifier, showing good results. *Zhang, et al.* [105] investigated the feasibility of Nafion/PTFE composite membranes with different kinds of porous PTFE substrates, showing that the Nafion/PTFE membrane was able to achieve higher through-plane conductivity than Nafion 117 at higher temperatures of 100 °C, demonstrating the potential for application in high-temperature conditions.

In recent years, various studies have explored modifications to Nafion membranes [109-113]. *Shin, et al.* [114] detailed their work on a perfluorinated composite membrane that incorporates organic antioxidants-Bipyridine (BPY) and Benzoquinone (BQ). These antioxidants were added to the Nafion solution at 25 ºC for 8 hours, constituting 2.5 mol% relative to the sulfonic acid content of Nafion. The preparation of composite membranes involved the solution casting method, and subsequent testing confirmed enhanced durability attributed to the introduction of organic oxidants. Following the Fenton test, the composite membrane with antioxidants exhibited fewer pinholes, a lower increase in turbidity, and a reduced emission rate of F ions compared to a pristine composite membrane. An OCV-holding test reveals that the perfluorinated electrolyte membrane containing organic antioxidants exhibited improved chemical durability, implying that its antioxidant capability is effective.

Mazzapioda, et al. [115] detailed the development of Nafion composite membranes enriched with TiO2-SO4 additives, synthesized using a sol-gel method. The study underscores the impact of additive concentration on the physical-chemical properties of the membranes. Impedance studies and fuel cell tests revealed a decrease in ohmic resistance and an enhancement in charge-transfer behavior. This suggests that even a minimal amount of sulphated titania has the potential to boost the performance of high-temperature proton exchange membrane fuel cells (HT-PEMFCs).

In a parallel effort, *oh, et al*. [116] engineered a Nafion composite membrane incorporating Silica Sulfuric Acid (SSA) filler particles. The resulting Nafion-SSA composite membrane demonstrated improved proton conductivity and fuel cell performance. Under 20% Relative Humidity (RH) conditions at 80 ºC, it achieved a 1.7 times higher proton conductivity than the reprocessed Nafion. Furthermore, under 25% RH conditions at 80 ºC, the membrane exhibited a peak power density of 454 mW cm^{-2} and a current density of 2,062 mA cm^{-2}, surpassing the reprocessed Nafion under the same conditions (159 mW cm^{-2} and 734 mA cm^{-2}, respectively). *Parnian, et*

al. [117] explored recast Nafion nanocomposite membranes loaded with zirconia nanoparticles. The addition of hygroscopic zirconia nanoparticles led to increased proton conductivity, higher water uptake, improved chemical durability, and enhanced mechanical properties. *J Choi, et al*. [118] introduced multifunctional dendritic Nafion/CeO_2 membranes, aiming to enhance the performance and durability of PEMFCs. By utilizing the electrospray deposition method, CeO_2 dendritic structures with high surface area and porosity were integrated onto the cathode side of the membrane. This approach improved mass transport of reactants, enhanced water retention capacity under low-humidity conditions, and ultimately contributed to enhanced fuel cell performance.

Vinothkannan, et al. [119] focused on Nafion/Fe_3O_4-SGO composite membranes for PEMFC applications. The addition of iron oxide (Fe_3O_4) anchored over Sulfonated Graphene Oxide (SGO) particles significantly increased water uptake, ion exchange capacity, proton conductivity, as well as mechanical and thermal properties. The composite membrane outperformed pristine Nafion in PEMFC performance tests. *Kannan, et al*. [120,121] reported on the introduction of sulfonic acid functionalized carbon nanotubes into the Nafion polymer matrix. The enhanced proton conductivity of the membranes was attributed to increased sulfonic acid content and the establishment of a channel-like network for proton transport. *Cele, et al*. [122] found that hybrid Nafion membranes containing 1 wt.% of oxidized carbon nanotubes exhibited improved thermal and mechanical characteristics compared to pristine Nafion membranes. *Steffy, et al*. [123] developed Nafion hybrid membranes with the incorporation of Sulfonated Multiwalled Carbon Nanotubes (sMWCNTs). These nanotubes, with sulfonic acid functional groups, improved compatibility with the polymeric matrix, enhancing mechanical and thermal stability. The sMWCNTs also increased water uptake capacity and proton conductivity, especially under reduced RH conditions. In PEMFC performance tests at 60 ºC and 20% RH, the composite membrane achieved a peak power density of 549 mW cm^{-2} at a load current density of 1.7 A cm^{-2}, surpassing the performance of the pristine recast Nafion membrane under the same conditions.

Also working on hybrid Nafion membranes with MWCNTs, *D Kim, et al*. [124] present their work on ultrathin MWCNTs/CeO_2 layers for Nafion reinforcement. In their work, it is said that the MWCNTs' dispersion characteristics were greatly improved by acid treatment, and a ball-milling procedure was carried out at 300 rpm for 12 hours to allow the CeO_2 nanoparticles to physically adhere to the MWCNTs' surface. Utilizing lab-made spray-coating equipment, the prepared mixed solutions were sprayed over a Nafion NR211 membrane to create ultrathin and highly dispersed MWCNTs/CeO_2 layers on the membrane surface. Despite the inclusion of nonconducting reinforcing materials, the modified NR211 with ~450 nm thickness MWCNTs/CeO_2 layers showed a proton conductivity loss of less than 3.4% while showing enhanced dimensional, mechanical, and chemical stability relative to those of the original NR211. Additionally, the ultrathin layers showed decreased hydrogen crossover as it served as an effective gas barrier at the membrane's surface. A 72-hour accelerated OCV holding test revealed that the MEA with the altered membrane had a modest drop in initial performance but greatly enhanced chemical durability by showing much slower OCV decay rates.

Protic Ionic Liquids (ILs), known for their ability to donate protons, have become a focal point in the quest for efficient proton conductors in PEMFCs. Utilized as electrolytes, either in blends or composites, these ILs demonstrate notable electrochemical and thermal stabilities, exhibiting high conductivities even in the absence of water at temperatures surpassing 100°C. These attributes expand the operational temperature range of fuel cells and enhance electrochemical performance, particularly in low-humidity conditions.

In a novel study by *Maiti, et al*. [125], a hybrid composite proton exchange membrane was developed by incorporating graphene oxide, dihydrogen phosphate functionalized imidazolium ionic liquid (IL-H_2PO_4), and Nafion 117 solution. The addition of IL-H_2PO_4 and graphene oxide improved the thermal stability of the Nafion membrane, and their concentrations, along with temperature, enhanced the membrane's ionic conductivity. At 110°C, under anhydrous conditions, the composite membrane achieved a remarkable ionic conductivity of 0.061 S cm^{-1}, 1.3 times higher than that of commercial Nafion 117. Furthermore, the Nafion/IL/GO membrane demonstrated a power density of 0.02 W/cm^2 at the same temperature, surpassing the pristine Nafion 117 membrane by 13 times.

Danyliv, et al. [126] delved into the potential of protic ILs, specifically N-ethylimidazolium trifluoromethylsulfonate ([EIm][TfO]) and N-ethylimidazolium bis(trifluoromethylsulfonyl)imide ([EIm][TFSI]), as charge carriers in modified Nafion membranes. Their study focused on understanding the nano- and microstructure changes in Nafion membranes swollen with various protic ILs and their impact on measured ionic conductivity. Despite the observed suppression of thermomechanical characteristics by ILs, the membranes exhibited substantial conductivities in the range of 0.2 to 1.2 × 10^{-3} Scm^{-1} at temperatures ranging from 90 to 150˚C.

For a distinct application, *fan, et al*. [127] conducted experimental research, showcasing the application of a PVDF-modified Nafion membrane in Microbial Fuel Cells (MFCs) designed for wastewater treatment. These bio-electrochemical fuel cells leverage redox reactions in living microbial cells to generate electric current. The incorporation of these membranes enhances the MFC's output voltage stability, exceeding 0.21 V, and boosts the removal rate of Chemical Oxygen Demand (COD) from wastewater by over 75% compared to MFCs employing conventional Nafion membranes.

In the realm of Nafion membranes for methanol fuel cell applications, *Ru, et al*. [128] explored the combination of sulfonated poly (arylene ether ketone) (SPAEK) and Nafion to create three distinct SPAEK@Nafion membranes with varying structures. The introduction of sulfonic acid groups, grafted onto the main and side chains of SPAEK using chlorine treatment, resulted in improved proton con-

ductivity compared to unmodified Nafion. Further advancements were achieved by incorporating a crosslinking agent, fluorinated epoxy resin monomer (fEO), leading to the creation of a semi-interpenetrating polymer network in the composite membrane (S@N/fEO) [129]. This modified membrane exhibited reduced methanol permeability and outperformed Nafion 212 by by about 1.3 times in terms of selectivity and Direct Methanol Fuel Cell (DMFC) performance.

Mazinani, et al. [130] developed three hybrid membranes-Nafion-calcium oxide (CaO), Nafion-zirconium phosphate (ZrOH), and Nafion-CaO-ZrOH-tailored for use in DMFCs. The incorporation of inorganic particles in these membranes significantly lowered methanol crossover by impeding transport. Nafion-CaO and Nafion-CaO-ZrOH exhibited a tenfold and sixfold enhancement in proton conductivity, respectively, compared to Nafion. The synergy of water uptake and novel proton hopping sites introduced by ZrOH contributed to the improvement in proton conductivity.

An alternative modification approach involved incorporating nanometer-sized hygroscopic inorganic acid, zirconium phosphate (ZrP), into Nafion. This method, presented by *Sun, et al*. [131,132], resulted in enhanced proton conductivity even at high temperatures due to the hydrophilicity of ZrP. The methanol permeability of Nafion/ZrP composite membranes was significantly reduced compared to pure Nafion. The methanol permeability of Nafion and Nafion/ZrP composite membranes is stated to be 8.84×10^{7} cm^2 s^{-1} and 0 cm^2 s^{-1}, respectively, at 5 M methanol solution and 60˚C. Zeolite has been extensively studied for DMFC applications due to its hydrophilic, ion-conductive, and highly crystalline properties. *Sun, et al*. [134] used zeolite UZM-9 in a Nafion composite membrane, creating a selective proton-sieving barrier that outperformed the original Nafion membrane in terms of power density and methanol permeation rate. *Cui, et al*. [135] incorporated NH4-X zeolite into a Nafion membrane, achieving improved proton conductivity and reduced methanol permeability. Submicron NH_4-X zeolites demonstrated better selectivity and a threefold increase in power density compared to pristine Nafion in DMFCs.

Prapainainar, et al. [136,137] explored the modification of Nafion membranes using Modernite (MOR) and Analcime (ANA) zeolites, observing lower methanol permeability and enhanced proton conductivity with MOR/Nafion compared to ANA/Nafion. The introduction of GO to modify MOR further improved performance, achieving higher power density and lower methanol permeability. Another study by *Prapainainar, et al*. [133] created a Nafion/silane-modified MOR composite membrane, yielding a MFC with 47% higher power density than the original Nafion membrane when fueled by 4 M methanol. These studies collectively highlight the diverse approaches and improvements made to Nafion membranes for various fuel cell applications, addressing issues such as methanol permeability, proton conductivity, and selectivity.

Sulphonated Trifluorostyrene (TFS) Membranes

The synthesis of the monomer α, β, β-trifluorostyrene was initially accomplished in the *1940s by Cohen, et al*. [138], who documented its complete synthesis. In the 1960s, Hogdon delved into the sulfonation of α, β, β-trifluorostyrene, exploring applications in structures and cells [139]. Through optimizing reaction conditions, he generated a variety of linear and crosslinked poly-α, β, β-trifluorostyrene sulfonic acids. Hogdon demonstrated that the challenging sulfonation of poly-α, β, β-trifluorostyrene was attributed to the beta-directing influence of the perfluorinated polyalkyl group attached to the aromatic ring [139]. Building upon the research on sulfonated α, β, β-trifluorostyrene membranes, a group of sulphonated copolymers incorporating α, β, β-trifluorostyrene and various substituted-α, β, β-trifluorostyrene comonomers was developed, collectively known as BAM3G (Ballard Advanced Materials third generation of membranes) [87,140]. The BAM3G membrane exhibited superior performance compared to both Nafion 117 and the Dow membrane at currents exceeding 0.6 A cm^{-2} [140,141]. It was anticipated that these membranes would be cost-effective polymer-based electrolytes, with production costs expected to align well with fuel cell applications. However, notable drawbacks include the intricate production process for the α, β, β-trifluorostyrene monomer and the challenging post-sulfonation procedures [139,142].

Radiation-Grafted Membranes

Essentially, radiation-induced processes involve changes in the intrinsic polymer properties when exposed to ionizing radiation. As the energies related to irradiation are significantly higher than the respective electron binding energy, it promotes bond cleavage and results in the formation of free radicals as well as crosslinks and end-links by the combination of these [143]. The first most significant work carried out on the radiation grafting of polymers was achieved and reviewed by Chapiro in the 1960s [144]. The cation exchange membrane has been prepared by graftpolymerising α, β, β-trifluorostyrene onto the inactive polymer (fluorine-containing polymer) film, and then sulphonating the grafted film in different patents. The grafted polymer membranes were obtained at a graft rate of 10 to 50%. Then, already in the 90s, styrene or α, β, β-trifluorostyrene was grafted onto-fluorine-containing polymers, followed by sulphonation of the grafted film. The reports [87,145] indicate that the oxidation stability of these grafted foils is very limited, thus making them appropriate only for fuel cell applications. Only the membranes based on the poly(tetrafluoroethylene) backbone showed some promise as a candidate material.

At the time, it has been claimed that another approach using the simultaneous and pre-radiation grating of monomers onto a base polymer film, and subsequent sulphonation of the grafted component, could be a viable method for synthesizing stable proton conducting membranes [146]. Membranes were prepared in different steps based on fluoropolymer films, such as poly (Tetrafluoroethylene-co-Hexafluoropropylene), FEP, or poly (Ethylene-Alt-Tetrafluoroethylene), ETFE. Nowadays these membranes are produced by established industrial processes, where the inexpensive commercial materials and a large degree of customization make them com-

petitive and attractive options [120]. The preparation procedure can be simplified into three steps (Figure 7), the pre-irradiation of the base matrix by ionizing sources, followed by the grafting of an advantageous monomer into the matrix, and to finish, the sulfonation of the grafted membrane. There are several examples of commercial radiation-grafted polymer membranes in the market, commercialized by companies such as Ashahi Glass Inc., Solvay, and Shanghai Shilong Hi-Techn. Corp. Ltd., to cite some [147]. There has been a focus on radiation grafting of substitute styrene monomers such as α, β, β-trifluorostyrene, and α-methylstyrene, in between others (Figure 8), in an attempt to improve the chemical stability of the membranes.

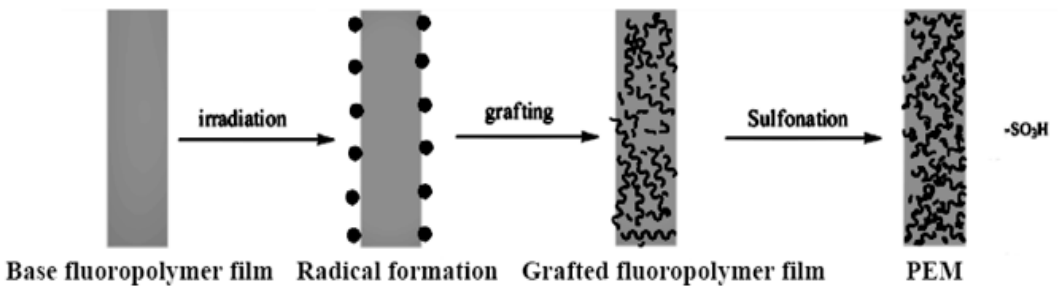

Figure 7: Multiple steps in the preparation of membranes by the radiation-grafting method.

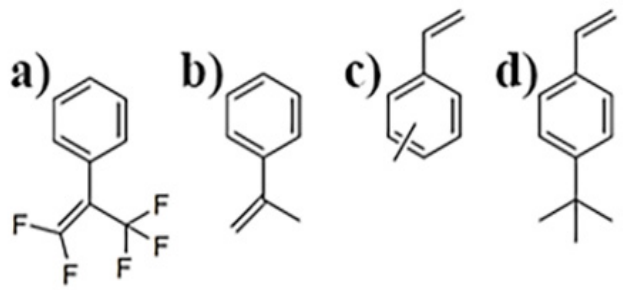

Figure 8: Styrene-derived monomers used in radiation-synthesized ion-exchange membranes, a) α, β, β-trifluorostyrene, b) α-methylstyrene, c) m, p-methylstyrene, and d) tert-butylstyrene.

FEP is an interesting material as the presence of a fluorinated matrix confers excellent resistance to aggressive media. Un-cross-linked FEP-g-PSSA membranes show high proton conductivity and cross-liked FEP-g-PSSA show negligible degradation at 80-85 ºC. However, uncross-linked FEP-g-PSSA membranes are susceptible to oxidative degradation, so alternative grafting monomers are employed to graft these films, increasing their durability over ten times at a temperature of 80 ºC [148]. *Li, et al*. [149] report on the production of FEP-g-PSSA films based on a 12.5 μm thick FEP film. The film was first immersed into 2.5 mol L-1 styrene in dichloromethane solution, in quartz tubes that were then radiated by 60Co. The dose rate was ranging from 10 kGy to 50 kGy. The films were then cleaned to get rid of residual monomer and polystyrene and dried at 60 ºC till constant weight. The resulting FEP-g-Polystyrene membrane was then sulfonated by chlorosulfonic acid (2 v/v% in 1,2-dichloroethane) at 40 ºC and hydrolysis in de-ionized water at 80 ºC for 8 h, to finalize the procedure. The membrane had a thickness of about 20-25 μm and exhibit excellent physicochemical properties. The membrane with 27.48% degree of graft, and 130.1 mS cm^{-1} proton conductivity, under operating conditions of 80 ºC and 75% relative humidity, reaches values of power density up to 0.896 W cm^{-2}. The study also shows that the mass-transport-controlled polarization of membrane electrode assembly (MEA) based on FEP-g-PSSA membrane is higher than Nafion 211 within the whole range of current densities tested. At 2.0 A cm^{-2}, the mass transfer polarization of FEP-g-PSSA reaches up to 0.204 V, much higher than the 0.084 V presented by Nafion 211. B. *Kim, et al*. [150] disclose the preparation of FEP films by pulsed electron beam direct grafting. A high-dose rate of radiation is applied to avoid undesired free radical homopolymerization of styrene and ensure uniform covalent grafting. At 80 ºC, the results show measured proton conductivity of 0.29 S cm^{-1} at 92% humidity, being at the same level as 3M 825 EW ionomer membrane and higher than the Nafion 112 membrane, and proton conductivity of 0.007 S cm^{-1} at 28% humidity, lower than both previously mentioned standard membranes. It is stated that this is due to sulfonated styrene having a higher pKa value than the PFSA membrane.

ETFE has garnered extensive attention and application as a foundational matrix for radiation grafting membranes due to its remarkable radiation stability and superior mechanical attributes. Two refined techniques in radiation-induced grafting have been devised to enhance the performance of ETFE-g-PSSA membranes. The initial method involves pre-treatment with heavy ion beams of $^{129}Xe^{23+}$ to create latent tracks traversing the ETFE film. Subsequent γ-ray pre-irradiation grafting of styrene results in membranes exhibiting proton conductivity in the thickness direction three times greater than in the surface direction. Styrene readily grafts in these latent track regions, forming conducting tunnels [151]. The second technique entails the selective exposure of the ETFE film to hard synchrotron X-rays through Ni-masks, forming patterns of free radicals that serve as initiators for the grafting of styrene/Divinyl Benzene (DVB). While this technique exhibits a slight performance reduction due to a lower active area, it presents a significantly longer lifetime attributed to less diffusion of oxidative chemical degradation species [152]. Presently, ETFE membranes prepared through radiation-induced graft copolymerization continue to undergo development and exploration, focusing on their synthesis, functional monomers, and the effects of irradiation [143,153-156].

Alternative fluoropolymer films commonly employed as foundational materials in the radiation synthesis of IEM for PEMFC applications encompass PTFE [157-165] and PVDF [166-168] films. The process of radiation-induced grafting on PTFE films may present challenges due to their vulnerability to radiation instability [147]. Reports suggest that the adoption of radiation-crosslinked PTFE (cPTFE) [157-160] or PTFE/PFA polymer blends [161] can notably bolster the radiation resistance of PTFE. Another viable approach involves UV-induced photo-grafting. Comparatively, PTFE-g-PSSA membranes resulting from UV-induced photo-grafting maintain conductivities akin to Nafion membranes, despite exhibiting a degree of grafting of less than 10% [162].

Acid Doped Polybenzimidazole (PBI) Membranes

Polybenzimidazole (PBI) (depicted in Figure 9) stands out as a synthetic polymer renowned for its remarkable thermal stability and commendable mechanical strength [147,169,170]. Initially discovered through the melt condensation process involving aromatic tetraamine, aromatic dicarboxylic acid, and aromatic dibasic acid, PBI's straightforward synthesis involves the solution polymerization of diamines and carboxylic acids in Polyphosphoric Acid (PPA) [169]. While the intrinsic proton conductivity of PBI ranges from 10^{-7} to 10^{-6} S cm^{-1}, doping it with an acid, particularly Phosphoric Acid (PA), significantly enhances proton conductivity, even in low humidity conditions, owing to PA's role as a proton carrier. PA-doped PBI has demonstrated an impressive proton conductivity of 7.9×10^{-2} S cm^{-1} at 5% RH and 200 ºC [171]. Among various acids tested for doping PBI at concentrations of 11 - 16 mol L^{-1}, the conductivity hierarchy is $H_2SO_4 > H_3PO_4 > HClO_4 > HNO_3 > HCl$. Despite sulfuric acid exhibiting superior conductivity, phosphoric acid proves less reliant on humidity, making it the preferred dopant in practical applications [169].

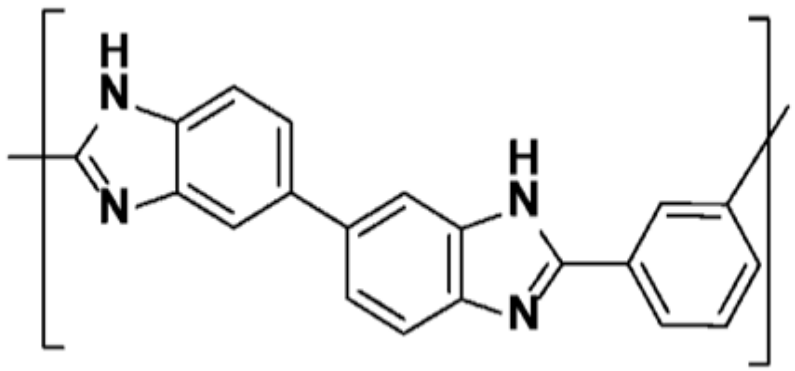

Figure 9: Molecular structure of m-PBI (poly[2,2-(m-phenylene)-5,5bibenzimidazole]).

The several advantages of PA-doped PBI prompted the researchers at Case Western University [172-175] to develop this membrane as a polymer electrolyte for methanol fuel cells in the 90s. They studied PBI films with two distinct casts. In the first case, they were cast from a solution of the polymer and then subsequently doped by immersion in a solution of 11 M PA for several days [172,175]. These films were referred to as type I films. The doping level was typically five PA molecules per repeat unit in a polymer-suitable solvent. In the second fashion, referred to as type II, films were cast from a polymer and phosphoric in a suitable solvent. In the second case, the sample preparation is greatly shortened as the films as the cast are already doped, with the typical doping level being six PA molecules per repeat unit in the polymer. It was shown that the conductivity of type I membranes increases with acid content, relative humidity, and temperature. The conductivity ranges between 0.01 - 0.04 S cm^{-1} for temperatures between 130 and 200 ºC and relative humidity of 0.04 - 0.4. For the type II membranes, the conductivities were higher. At temperatures above 150

ºC, the conductivity of these membranes is similar to that of Nafion at 80 ºC and 100% RH. They have shown that the methanol crossover through type I membranes was at least ten times less than that observed with Nafion. It was claimed that the electroosmotic coefficient of water drag determined under different conditions (temperature, humidity, and current density) was essentially zero. It was anticipated that the water balance problems should not appear with fuel cells using PBI membranes. For direct methanol fuel cells, the type II cell produced 0.21 W cm^{-2} at 500 mA cm^{-2}, as compared to 0.16 W cm^{-2} for the cells with type I membrane, a tolerance of 1% CO in H_2 was found due to the lower CO adsorption at this temperature [175]. These studies seem to indicate that PA-doped PBI membranes are promising candidates for use in HT-PEMFCs. However, some of the disadvantages of these systems doped with PA are related to the leaching of the PA, poisoning of the cathode Pt electrocatalyst with PA, self-dehydration of PA above 140 ºC, and low mechanical stability at high PA concentrations [147,169,170]. Therefore, many hybrid materials are nowadays being developed such as through crosslinking methods, modification of polybenzimidazole structure, or addition of inorganic proton conducting materials to try to solve these problems and improve the performance of these materials [114,160,161,175-177].

L. Wang, et al. [178] delve into the impact of branching structures on PBI's properties as a membrane in fuel cells. Employing the solution casting method, three distinct types of branched PBIs were prepared as HT-PEMs. Results indicate that the introduction of a branched structure enhances the processability, proton conductivity, oxidative stability, and fuel cell performance of the PBI membranes. The study emphasizes that the bulk rigid branched structure significantly contributes to the overall membrane performance. *Haque, et al*. [179] conduct an investigation on H_3PO_4-PBI copolymers, drawing comparisons with other solid electrolyte membranes (SEMs) for HT-PEMFC applications. The most promising PBI copolymer exhibits a proton conductivity of 5.29 mS cm^{-1}, demonstrating commendable chemical and mechanical strength along with excellent thermal resistance.

In recent developments, ionic liquids (ILs) emerge as a potential solution for addressing the conductivity challenges of PBI membranes, which are contingent on acid concentration. Due to the proton donors and acceptors in their chemical structures, ILs have the capability to enhance the conductivity of PBI monomers even in low Phosphoric Acid (PA) concentrations [180]. *Gao, et al*. [181] outline the synthesis and characterization of PBI membranes with hyper-branched cross-linkers adorned with imidazolium groups (ImOPBI-x). These branched polymers exhibit notable oxidative stability, heightened proton conductivity, and reduced loss of PA molecules compared to linear polymers. *Liu, et al*. [182,183] contribute to this area by developing different series of cross-linked fluorine-polybenzimidazole (6FPBI) membranes with the incorporation of ILs. The application of cross-linked polymeric IL compounds is suggested in the first work, where the anions in the polymeric ILs form rapid channels for proton transfer, preventing IL compound leakage. In the more recent work, highly conductive cross-linked membranes, comprising 6FPBI and poly (ionic liquid) (PIL) through in situ free radical polymerization and cross-linking, are presented. The PIL is prepared by mixing 1-vinylimidazole with 1-chlorobutane. These membranes exhibit improved PA stability (up to 73.1% at 400 h under 160 ºC, 0% RH), enhanced mechanical properties, and elevated proton conductivity (0.069 S cm-1 at 170 ºC). *Escorihuela, et al*. [184] unveil the development and characterization of composite PBI membranes containing zeolitic imidazolate frameworks 8 (ZIF-8) and 67 (ZIF-67). The addition of ZIF to the polymeric matrix enhances proton transport, with PBI@ZIF-8 and PBI@ZIF-67 membranes achieving proton conductivities of 3.1×10^{-3} S·cm^{-1} and 4.1×10^{-2} S·cm^{-1}, respectively, at 200 °C. A composite membrane with a 5 wt.% binary mixture of ZIF-8 and ZIF-67 yields a proton conductivity of 9.2×10^{-2} S·cm^{-1}, surpassing individual ZIF-containing membranes, suggesting a synergistic effect on proton conductivity. *Rajabi, et al*. [185] provide insights into the effects of SBA-15 mesoporous structures on the properties of H3PO4-doped PBI/IL membranes for high-temperature fuel cell applications. The introduction of PAMAM mesoporous structures is highlighted to enhance proton conductivity stability in composite membranes, ultimately improving the performance of HTFCs during long-term operations.

Sulphonated Polyimide (SPI) Membranes

These sulfonated polyimides are derived from 4,4'-diaminobiphenyl 2,2'-disulphonic acid (BDSA), 4,4'-oxydianiline (ODA), 4,4'-oxydiphthalic anhydrides (OPDA), and 1,4,5,8-naphthalene tetracarboxylic dianhydride (DNTA). In the 1990s, *Cornet, et al*. [186] conducted a study on these membranes, exploring the swelling and conductive properties of naphthalenic Sulfonated Polyimide (SPI) membranes based on the ionic content and ion distribution along the polymer chain. The findings, considering the anisotropy of the microstructure, nanoscale existence, and a microstructure composed of hydrophobic domains embedded in a continuous ionic phase of ionic sticks, led to the conclusion that SPI ionomers could be classified as a new class of Ion Exchange Membranes (IEM). Subsequent studies in the following decade, particularly on their application in Direct Methanol Fuel Cells (DMFC), emphasized the suitability of these membranes due to their high thermal stability, elevated proton conductivities, and comparatively low methanol permeability compared to Nafion membranes [187,188].

Currently, several strategies have been developed to enhance the hydrolytic stability of sulfonated polyimides [147]. Notably, SPI blendings with inorganic particles and cross-linked PEMs based on branched SPIs have garnered attention for their superior performance compared to other membranes, including Nafion. *You, et al*. [189] detail an SPI composite membrane modified with a bio-filler derived from rice husk waste, rice husk ash (RHA). This SPI-RHA composite membrane exhibits a proton conductivity of 0.2058 S cm^{-1}, surpassing that of a pristine SPI membrane. Furthermore,

the methanol permeability of the SPI-RHA membrane is 24 times lower than that of the pristine SPI membrane. In a DMFC passive single-cell test using a composite membrane with 15 wt.% RHA, a maximum power density of 13.0 mW cm^{-1} was achieved, an improvement from 8.0 mW cm^{-1}. These findings underscore the significant potential of RHA as a cost-effective alternative method to enhance membrane performance for fuel cell applications. In another approach, *Hu, et al*. [190] reveal a novel method for producing cross-linked membranes containing a branched structure, demonstrating higher power density (53.4 mW cm^{-2}) compared to conventional cross-linked membranes (43.0 mW cm^{-2}). These membranes exhibit excellent chemical stability, mechanical properties, and fuel cell performance, indicating ongoing opportunities for the development of high-performance materials based on SPIs for fuel cell applications.

Styrene/Ethylene-butadiene/Styrene (SEBS) Triblock Copolymer Membranes

The styrene/ethylene-butadiene/styrene triblock polymer is a commercially available product, containing a saturated carbon centre block, which should be inert to the sulphonation reaction. DAIS Company (USA) developed these membranes in the 90s as a less expensive alternative to Nafion [191]. SEBS is obtained by the full hydrogenation reaction of thermoplastic elastomer Styrene-Butadiene-Styrene (SBS). The full hydrogenation of SBS prevents undesirable side reactions in the non-aromatic double bonds, wielding high degrees of functionalization in SEBS, which is necessary to achieve adequate proton conductivity values.

Nowadays, SEBS still is one of the promising materials for membrane separators due to its high thermal, chemical, and tunable mechanical properties, cost-effectiveness, and promising proton conducting properties [192]. Recently many studies have been performed on PEMs based on SEBS prepared via sulfonation, grafting, and crosslinking methods. *Park, et al*. [192] document a sulfonated poly(styrene-ethylene-butylene-styrene) copolymer (S-SEBS), further modified with sulfonic acid groups and grafted with maleic anhydride (S-SEBS-g-MA) to improve the ionic conducting proprieties. The electrochemical analysis revealed that the modified membranes showed ionic conductivity of 0.25 S cm^{-1} at 100% relative humidity, with 72.5% water uptake capacity and without observable changes in their mechanical and chemical properties, revealing the robustness of the modified SEBS membranes. At room temperature, the ionic conductivity, water uptake, and ionic exchange capacity of the S-SEBS, SEBS-g-MA, and S-SEBS-g-MA membranes were shown to be higher than those of the commercial Nafion 117 membrane, revealing that these this method could open alternative strategies and promising approaches for further development. *Juanes, et al*. [193] present a set of SEBS triblock copolymer membranes with Divinyl-Benzene (DVB) as a crosslinking agent. The physicochemical characterization reports on photo-crosslinked membranes containing 25 wt.% DVB, with hydrolytic and thermal stability suitable for application in PEFCs. The membranes with the milder post-sulfonation showed greater proton conductivity than those with excessive sulfonation and in terms of electrical conductivity, the results shown support the use as polyelectrolytes. The fuel cell performance revealed the best behaviour for the membrane with 25 wt.% DVB, photo-crosslinked during 30 min and mild sulfonated, with a power density of 526 mW cm^{-2}.

Sulphonated Poly (Arylene Ether Sulphone) (SPAES) Membranes

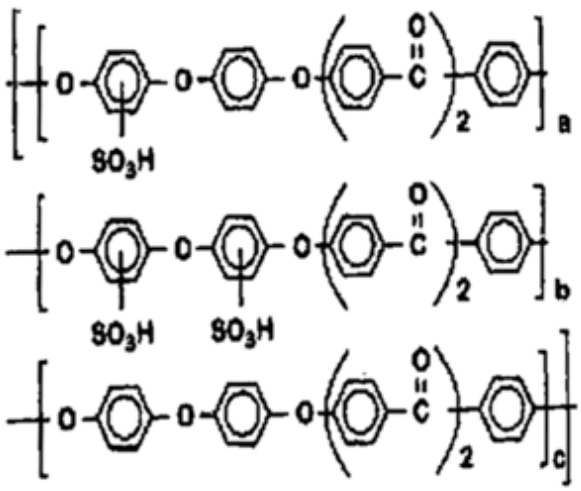

Figure 10: General chemical structure of polyether ether ketone (PEEK).

The synthesis and characterization of sulphonated poly (arylene ether sulphones) conducted in the 60s demonstrated excellent mechanical properties, thermal stability, toughness, and resistance to hydrolysis and oxidation [194,195]. However, the electrochemical properties of these membranes were not investigated at that time. In the present day, poly (arylene ether)-based membranes have emerged as one of the most promising alternative Proton Exchange Membranes (PEMs) due to their favourable attributes, including availability, processability, outstanding thermal and chemical stability, good mechanical properties, and cost-effectiveness. In these membranes, sulfonic acid groups serve as proton-exchange sites and are more commonly utilized and studied due to their ease of introduction into aromatic rings compared to other acids like carboxylic or phosphonic acids [147]. Nonetheless, challenges arise in the practical application of sulphonated poly (arylene ether sulfones) (SPAES) membranes, as a high degree of sulfonation for enhanced proton conductivity leads to excessive swelling and reduced thermal stability. On the other hand, cross-linked membranes created by covalent bonds may enhance chemical and dimensional stability but often at the expense of proton conductivity [196,197]. Addressing these challenges, the incorporation of inorganic particles has been identified as a crucial factor for improving mechanical strength and methanol permeability without compromising ion conductivity. Studies on the production of organic-inorganic composite membranes by adding materials such as silica, clay, metal oxides, and carbon nanotubes have shown promise, particularly with clays contributing to enhanced proton conductivity, water uptake, and thermal and mechanical strength [196,197].

Kim, et al. [198] present a method for preparing a high-performance cross-linked sulphonated poly (arylene ether sulfone) (C-SPAES) membrane for fuel cell applications. The use of a flexible bishydroxy Perfluoropolyether (PFPE) as a cross-linker improves physicochemical stability and proton conductivity. The resulting electrode assembly demonstrates high cell performance of 1.17 W cm^{-2} at 0.65 V under working conditions of 90 ºC, 150 kPa, and 50% RH. *Choi, et al*. [199] explore the impact of an aliphatic moiety in the backbone of sulfonated poly (arylene ether sulfone) (SPAES). Partially alkylated SPAESs were synthesized using the monomer 4,4'-dihydroxy-1,6-diphenoxyhexane, and a cell prepared with this membrane exhibits a peak power density of 539 mW cm^{-2}. In a recent publication, *J Kim, et al*. [200] detail the preparation of PAES block copolymers through a condensation polymerization reaction, resulting in membranes with high conductivity and alkaline stability, achieving a power output of 64 mW cm^{-2} in single-cell tests. Despite favorable physical-chemical characteristics, further improvements are needed in the power output and durability of the membrane.

Sulphonated Poly (Ether Ether Ketone) (SPEEK) Membranes

SPEEK membranes are widely studied and used as their original polymer, poly (Ether Ether Ketone) (PEEK), is commercially available and has important properties similar to those of many classes of aromatic polymers [147]. The structure of Polyether Ether Ketone (PEEK) is shown in (Figure 10) and consists of 1,4-disubstituted phenyl groups separated by any of several linkages of –O– and –CO– [O – (Ar) – O – (Ar) – CO – (Ar)–]n. The general formula of the aromatized polyether ether ketone is [201]:

[– [Ar – O]p – [Ar – [CO – Ar']x – O – Ar]m – [–CO – Ar']y – [O – Ar –]n –CO–]

where Ar is a phenyl group and Ar' may be phenyl, naphthyl, biphenyl, anthryl, or other aromatized groups. The value of x, n, and m can be 0 or 1. The value of y might be 0, 1, 2, or 3, and p of 0, 1, 2, 3, or 4. SPEEK membranes were initially proposed as proton conductors in polymer electrolyte fuel cells back in 1993 by *Schmeller, et al* [201]. However, contemporary challenges associated with SPEEK membranes are well recognized, including brittleness at elevated temperatures, excessive swelling, and relatively high methanol crossover, particularly in highly sulfonated membranes, leading to compromised durability. Despite these issues, efforts have been made to enhance membrane durability through modifications, such as cross-linking or radiation grafting methods [147,202-207].

Parnian, et al. [205] explored the impact of various Degrees of Sulfonation (DS) on the thermal, mechanical, and oxidative stabilities, water uptake behavior, and ionic exchange capacity of the membranes. The findings indicate an increase in proton conductivity with rising DS, albeit at the expense of reduced mechanical, thermal, and chemical stabilities. Membranes with a DS of 65% were deemed most suitable, maintaining acceptable physical-chemical properties and robust proton conductivity. Similar DS values for SPEEK membranes were reported by *Sun, et al*. [206]. *Wu, et al*. [207] engineered SPEEK core-shell nanofibers incorporating sulfonated organosilane graphene oxide (SSi-GO) through coaxial electrospinning, comparing their properties and performance with other SPEEK and Nafion membranes. The SSi-GO formed a distinctive cambiform-like morphology with micro-voids, contributing to increased water uptake. The SSi-GO/SPEEK membrane produced by electrospinning exhibited higher water uptake, proton conductivity, and methanol permeability than membranes produced by blend casting and mono-spinning methods. The hydrogen permeability was 39% of that of Nafion 115, even though it was thinner, and the methanol selectivity was 6.8 x 10^5 S cm^{-3}, approximately 11 times that of Nafion 115 (around 6.12 x 10^4 S cm^{-3}). *Pasquini et al*. [208] conducted a study on the hydrolytic stability, conductivity, and mechanical stability of different membranes based on SPEEK (and Sulfonated Poly (Phenyl Sulfone), SPPSU) ionomers with various casting solvents, including DMSO, water, and ethanol. Notably, the addition of SPPSU to SPEEK membranes improved their ionic conductivity. Comparisons with Nafion revealed that DMSO-cast SPEEK membranes exhibited higher conductivity and mass uptake.

Poly (Vinyl Alcohol) (PVA) Membranes

In the 1920s and 30s, *Herrmann et al*. documented the synthesis of Poly (Vinyl Alcohol) (PVA) (Figure 11) through various

methods, including saponification [209] and transesterification reactions with alkali catalysts [210], starting from poly (vinyl esters). In contemporary settings, PVA is predominantly produced on an industrial scale through the polymerization of vinyl esters or ethers, typically using vinyl acetate, followed by saponification or transesterification reactions [211]. Notably, *Cussler, et al*. [212] highlighted PVA membranes as superior barriers to methanol compared to Nafion membranes due to their selectivity for water over alcohols. However, PVA lacks negative-charged ions, such as carboxylic or sulfonic acid groups, making it a poor proton conductor. To enhance proton conductivity, a crosslinking agent containing negative-charged ions can be employed. Crosslinking also alters other properties of the base polymer, including water-uptake capacity, swelling degree, as well as thermal, chemical, and mechanical stability [113]. Various acids, such as citric acid, maleic acid, boric acid, and poly (acrylic acid), are commonly used in chemical crosslinking reactions with PVA [114,115]. While irradiation and heat treatment are alternative crosslinking methods, chemical crosslinking is generally preferred for PEM applications due to its ability to offer a broader range of control over desired characteristics, such as proton conductivity, in the host polymer [213, 216].

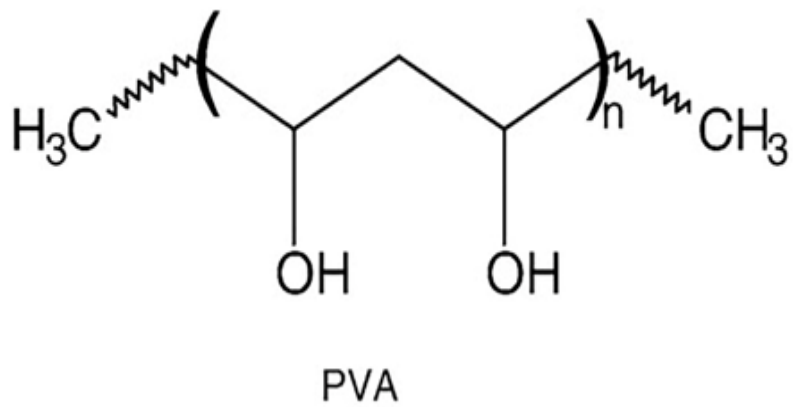

Figure 11: General chemical structure of Poly (Vinyl Alcohol) (PVA).

Rhim, et al. [217] explored crosslinked PVA membranes incorporating Sulfosuccinic Acid (SSA), revealing proton conductivities ranging from 10^{-3} to 10^{-2} S cm^{-1} and superior methanol barrier properties compared to Nafion 117. The straightforward procedure involves adding SSA (5 - 30 wt.%) to the PVA solution before membrane casting. Interestingly, methanol transport through the PVA/SSA membrane increased with SSA content beyond 17%. In a parallel investigation, *Hou, et al*. [218] observed an enhancement in the ion exchange capacity of PVA/SSA membranes with increasing SSA until a certain threshold. Surprisingly, 20 wt.% SSA resulted in lower proton conductivity than 15 wt.% SSA, a trend echoed in PVA-based crosslinked membranes using sulfoacetic acid as the crosslinker and proton source [219].

An alternate approach to enhance PVA membrane properties for fuel cell applications involves quaternization. Grafting PVA with ammonium quaternary functional groups enhances membrane conductivity properties and swelling ratios [220]. Among several quaternization processes, the one involving glycidyl trimethylammonium chloride and potassium hydroxide with PVA is commonly used [220]. *Kumar, et al*. [221] introduced perovskite $LaFeO_3$ nanofillers into the Quaternized PVA (QPVA) membrane matrix, resulting in lower methanol permeability and higher ionic conductivity. *Lin, et al*. [222] incorporated Fe3O4@GO magnetic nanoparticles into QPVA, achieving improved performance. *Gouda et al*. [223] developed a composite membrane based on crosslinked PVA/poly (ethylene oxide) (PEO)/poly (vinyl pyrrolidone) (PVP) ternary blend doped with sulfonated graphene oxide (SGO) for direct borohydride fuel cells (DBFC). The composite membrane demonstrated lower borohydride permeability than Nafion 117, with a peak power density matching that of Nafion 117 under the same conditions. Another novel PVA membrane crosslinked with Polyethylene Oxide (PEO) and doped with 3 wt.% phosphated titanium oxide (PO_4TiO_2) nanotubes showed enhanced oxidative stability, tensile strength, and lower fuel permeability compared to Nafion117 [224]. Studies with PVA/Graphene Oxide (GO) membranes revealed proton conductivities of 3.24×10^{-2} S cm^{-1} and a peak power density of 5.48 mW cm^{-2} for a passive direct ethanol-PEMFC at 60 ºC, surpassing those obtained with Nafion 117 (4.52 mW cm^{-2}) [225]. Given their attributes, such as low fuel crossover and permeability, robust ion conductivity, and excellent mechanical, chemical, and thermal stability, PVA-based membranes have garnered significant attention in recent years [226-228].

Conclusions

When Christian Friedrich Schoenbein and William Robert Grove made their discoveries in 1838 and 1845, respectively, they did not expect that undoubtedly nearly two centuries later they would be so strongly recognized as they are today. In fact, the fuel cell, and particularly the PEMFC, converting hydrogen to electricity without polluting the environment, is the chief enabler of the new age of <Distributed Generation>. Electric power is produced where it is needed. No energy is lost by transmission and the waste heat can readily be utilized. It may even take a substantial portion of the USD 300 billion approximately spent annually on internal combustion engines. Here we deal with the PEMFC and its applications and issues in the transport sector. Accordingly, the cell system is examined and answered and unanswered questions which emerge, are reported.

An important issue associated with the required development of the cells is concerned with the polymer electrolyte materials, and this article also deals with 9 key classes of polymer electrolytes-perfluorinated, sulphonated trifluorostyrene, radiation grafted, acid-doped polybenzimidazole, sulphonated polyimide, styrene/ethylene-butadiene/styrene, sulphonated poly(arylene ether sulphone), sulphonated poly(ether ether ketone) and poly(vinyl alcohol) membranes, which offer many advantages in the area of fuel cells for electric vehicles applications.

Acknowledgements

None.

Conflict of Interest

None.

References

1. Rourke D, Connolly S (2003) just oil? The distribution of environmental and social impacts of oil production and consumption. Annual Reviews of Environmental Resources 28(5): 587-617.
2. Sun C, Negro E, Vezzù K, Pagot G, Noto VD (2019) Hybrid inorganic-organic proton- conducting membranes based on SPEEK doped with WO3 nanoparticles for application in vanadium redox flow batteries. Electrochimica Acta 309: 311-325.
3. Weiss MA, Heywood JB, Drake EM, Schafer A, Au Yeung FF, et al. (2000) On the road in 2020: A life-cycle analysis of new automobile technologies. USA.
4. Larminie J, Dicks A (2003) Fuel Cell Systems Explained. John Wiley Sons Ltd Chichester UK.
5. Sun C, Negro E, Nale A, Pagot G, Vezzù K, et al. (2021) An efficient barrier toward vanadium crossover in redox flow batteries: The bilayer [Nafion/(WO3) x] hybrid inorganic-organic membrane. Electrochimica Acta 378: 138133.
6. Higa M, Atemura K, Sugita M, Maesova S, Endo N (2012) Performance of passive direct methanol fuel cell with poly (vinyl alcohol)-based polymer electrolyte membranes. International J Hydrogen Energy 37(7): 6292- 6301.
7. Maiyalagan T, Saji VS (2017) Electrocatalysts for Low Temperature Fuel Cells: Fundamentals and Recent Trends. Wiley-VCH UK.
8. Sequeira CAC (2019) High Temperature Corrosion: Fundamentals and Engineering. John Wiley & Sons, USA.
9. O'hayre R, Cha SW, Prinz FB, Colella W (2016) Fuel Cell Fundamentals, John Wiley & Sons, London UK.
10. Wilberforce T, El Hassan Z, Khatib FN, Makky A Al, et al. (2017) Developments of electric cars and fuel cell hydrogen electric cars. Int J Hydrogen Energy 42: 25695-25734.
11. Chandan A, Hattenberger M, El Kharouf A, Du S, Dhir A, et al. (2013) High temperature (HT) polymer electrolyte membrane fuel cells (PEMFC). A review J Power Sources 231: 264-278.
12. Mamlouk M, Sousa T, Scott K (2011) A high temperature polymer electrolyte membrane fuel cell model for reformate gas. Int J Electrochemistry.
13. Authayanum S, Wiyaratn W, Assabumrungrat S, Arpornwichanop A (2013) Theoretical analysis of a glycerol reforming and high temperature PEMFC integrated system: Hydrogen production and system efficiency Fuel 105: 345-352.
14. Authayanum S, Mamlouk M, Scott K, Aspornwichanop A (2013) Comparison of high-temperature and low-temperature polymer electrolyte membrane fuel cell systems with glycerol reforming process for stationary applications. Applied Energy 109: 192-201.
15. Qi Zhigang (2017) Proton Exchange Membrane Fuel Cells.
16. Schmittinger W, Vahidi A (2008) A review of the main parameters influencing long-term performance and durability of PEM fuel cells. J Power Sources 180: 1-14.
17. Buchi MIFN, Schmidt TJ (2009) Polymer Electrolyte Fuel Cell Durability. New York.
18. Santos E, Schmickler W (2007) Electrocatalysis of hydrogen oxidation - theoretical foundations. Angew. Chem Int 46: 8262-8265.
19. Hyun K, Lee JH, Yoon CW, Kwon Y (2013) The effect of platinum based bimetallic electrocatalysts on oxygen reduction reaction of proton exchange membrane fuel cells. International Journal of Electrochemical Science 8: 11752-11767.
20. Steele, BCH, Heinzul A (2001) Materials for fuel-cell technologies. Nature 414: 345-352.
21. Becker H, Bacquart T, Perkins M, Moore N, Ihonen J, et al. (2020) Operando characterization of the impact of carbon monoxide on PEMFC performance using isotopic labelling and gas analysis. J Power Sources Advances 6: 100036.
22. Seo, A, Lee J, Han K, Kim H (2006) Performance and stability of Pt-based ternary alloy catalysts for PEMFC. Electrochimica Acta 52: 1603-1611.
23. Knudsen BP, Chorkendorff I, Stephens I (2016) Synthesis of Platinum Rare Earth Alloy Catalysts for Fuel Cells. Denmark.
24. Yoshida T, Kojima K, Toyota Mirai (2015) fuel cell vehicle and progress toward a future hydrogen society. The Electrochemical Society Interface 24: 45-49.
25. Sequeira CAC (2014) Amaral L Bipolar plates for PEMFCs. Journal of Fuel Cell Science and Technology 11(4): 044001.
26. Shui J, Wang M, Du F, Dai L (2015) N-doped carbon nanomaterials are durable catalysts for oxygen reduction reaction in acidic fuel cells. Science Advances 1: e1400129.
27. Wang MQ, Yang WH, Wang HH, Chen C, et al. (2014) Pyrolyzed Fe-N-C composite as an efficient non-precious metal catalyst for oxygen reduction reaction in acidic medium. ACS Catalysis 4(11): 3928-3936.
28. Yang S, Xue X, Liu X, Liu W, Bi J et al. (2019) Scalable synthesis of micromesoporous iron-nitrogen-doped carbon as highly active and

stable oxygen reduction electrocatalyst. ACS Applied Materials & Interfaces 11 (42): 39263-39273.

29. Sequeira CAC, Santos DMF (2012) Electrochemical behavior of oxygen reduction on polymer carbon electrodes in alkaline media. Russian Journal of Electrochemistry 48(7): 801-811.

30. Chandran PC, Ghosh A, Ramaprabhu S (2018) High-performance platinum-free oxygen reduction reaction and hydrogen oxidation reaction catalyst in polymer electrolyte membrane fuel cell. Scientific Reports 8: 3591.

31. Zhang J, Li M, Guo P, Ma H, Zhao S (2016) Rational design of graphitic carbon-based nanostructures for advanced electrocatalysis. Journal of Materials Chemistry A 4: 8497-8511.

32. Schwämmlein JN, Harzer GS, Pfändner P, Blankenship A, El-Sayed HA, et al. (2018) Activity and stability of carbon supported PtxY alloys for the ORR determined by RDE and single-cell PEMFC measurements. Journal of The Electrochemical Society 165(15): J3173-J3185.

33. Qin J, Zhang Y, Leng D, Yin F, The enhanced activity of Pt-nanoalloy for oxygen electroreduction. Scientific Reports 2020 10: 14837.

34. Vietanti F, Wang CH (2020) PdFeCo supported on N-rGO as bifunctional catalyst for methane oxidation and high stability oxygen reduction reaction. Journal of Energy Mechanical Material and Manufacturing Engineering 5: 29-36.

35. Bu L, Tang C, Shao Q, Zhu X, Huang X (2018) Three-dimensional Pd3 Pb nanosheet assemblies: Highperformance non-Pt electrocatalysts for bifunctional fuel cell reactions. ACS Catalysis 8: 4569-4575.

36. Tang Y, Zhang H, Ma Y (2011) A facile synthesis of Pd/C cathode electrocatalyst for proton exchange membrane fuel cells. International Journal of Hydrogen Energy 36: 725-731.

37. Wang H, Qiu X, Wang W, Jiang L, Liu H (2019) Iron sulfide nanoparticles embedded into a nitrogen and sulfur co-doped carbon sphere as a highly active oxygen reduction electrocatalyst. Frontiers in Chemistry 7: 855.

38. Antolini E, Perez J (2011) The use of rare earth-based materials in low-temperature fuel cells. International Journal g Hydrogen Energy 36: 15752-15765.

39. Kim S, Kato S, Ishizaki T, Li OL, Kang J (2019) Transition metal (Fe, Co, Ni) nanoparticles on selective amino-N-doped carbon as high-performance oxygen reduction reaction electrocatalyst. Nanomaterials 9(5): 742.

40. Shinagawa T, Garcia-Esparza AT, Takanabe K (2015) Insight on Tafel slopes from a microkinetic analysis of aqueous electrocatalysis for energy conversion Scientific Reports 5: 10.1038.

41. Wang Y J, Zhao N, Fang B, Li H, et al. (2015) Carbon-supported Pt-based alloy electrocatalysts for the oxygen-reduction reaction in polymer electrolyte membrane fuel cells: particle size, shape, and composition manipulation and their impact to activity. Chemical Reviews 115(9): 3433-3467.

42. Shaari N, Kamarudin SK (2017) Graphene in electrocatalyst and proton conducting membrane in fuel cell applications: An overview. Renewable and Sustainable Energy Reviews 69: 862-870.

43. Van Pham C, Klingele M, Britton B, Vuyyurn KR, et al. (2017) Tridoped reduced graphene oxide as a metal-free catalyst for oxygen reduction reaction demonstrated in acidic and alkaline polymer electrolyte fuel cells. Advanced Sustainable Systems 1: 1600038.

44. He Cheng (2019) Corrosion-resistant non-carbon electrocatalyst supports for proton exchange membrane fuel cells. PhD Thesis. University of Washington in St. Louis Missouri.

45. Sharma S, Pollet BG (2012) Support materials for PEMFC and DMFC electrocatalysts. Journal of Power Sources 208: 96-119.

46. Zhao Y, Peng L (2019) Formability and flow channel design for thin metallic bipolar plates in PEM fuel cells: modeling. International Journal of Energy Research 43(7): 2592-2604.

47. Khatir FA, Elyasi N, Ghadikolaee TH, Hosseinzadeh M (2017) Evaluation of effective parameters on stamping of metallic bipolar plates. Procedia Engineering 183: 322-329.

48. Modanloo V, Alimirzaloo V, Elyasi M (2020) Optimal design of stamping process for fabrication of titanium bipolar plates using the integration of finite element and response surface methods. Arabian Journal for Science and Engineering 245: 1097-1107.

49. Alo OA, Otunniyi IO, Pienaar H (2019) Manufacturing methods for metallic bipolar plates for polymer electrolyte membrane fuel cell. Materials and Manufacturing Processes 34(8): 927-955.

50. Freris L, Infield D (2017) Renewable Energy in Power Systems. John Wiley & Sons, West Sussex U.K. 2008.

51. Wilson A, Kleen G, Papageorgopoulos D, Fuel Cell System Cost- 2017, DOE Hydrogen and Fuel Cells Program, Record number 17007: 2017.

52. Jendras P, Lotsch K, von Unwerth T (2017) Requirements and testing methods for surfaces of metallic bipolar plates for low temperature PEM fuel cells. Mater Sci Eng.

53. Kahraman H, Orhan MF (2017) Flow field bipolar plates, in a proton exchange membrane fuel cell: Analysis & modeling. Energy Conv & Management 133: 363-384.

54. Gao Y, Jin T, Wu X (2020) Stochastic 3D carbon cloth GDL reconstruction and transport prediction Energies 13: 572.

55. Jagur Grodzinski J (2007) Polymeric materials for fuel cells: concise review of recent studies. Polymers for Advanced Technologies 18: 785-799.

56. Quartarone E, Angioni S, Mustarelli P (2017) Polymer and composite membranes for proton-conducting, high-temperature fuel cells: A critical review Materials 10(7): 687.

57. Francia C, Ijeri VG, Specchia S, Spinelli P (2012) Estimation of hydrogen crossover through Nafion membranes in PEMFCs. Journal of Power Sources 196: 1833-1839.

58. Hotupally S (2007) International Workshop on Degradation Issues of Fuel Cells, Creta, Greece.

59. Gurau V, Mann IA (2009) A critical overview of computational fluid dynamics multiphase models for proton exchange membrane fuel cells. SIAM J Appl Math 70(2): 410-454.

60. Wan, CY (2004) Fundamental models for fuel cell engineering. Chem Rev 104 (10): 4727-4766.

61. Siegel C (2008) Review of computational heat and mass transfer modeling, in polymer-electrolyte membrane (PEM) fuel cells Energy 33(9): 1331-1352.

62. Djilali N (2007) Computational modelling of polymer electrolyte membrane (PEM) fuel cells: challenges and opportunities Energy 32(4): 269-280.

63. Wang Y, Basu S, Wang CV (2008) Modeling two-phase flow in PEM fuel cell channels J. Power Sources 179 (2): 603-617.

64. George D, Suresh PV (2016) Detailed analysis of integrated steam ethanol reformer and high temperature polymer electrolyte membrane fuel cell. Int J Hydrogen Energy 41: 1248-1258.

65. Shamardina O, Chertovich A, Kulikovsky AA, Khokhlov A (2010) A simple model of a high temperature PEM fuel cell. Int J Hydrogen Energy 35 :9954-9962.

66. Hengge K, Gansler T, Pizzutilo, E, Heinzl C, Beetz M, et al. (2017) Accelerated fuel cell tests of anodic Pt/Ru catalyst via identical location TEM: New aspects of degradation behavior. Int J Hydrogen Energy 42 :25359-25371.

67. Etesami M, Mehdipour Ataei S, Somwangthanaroj A, Kheawhorn S (2021) Practical aspects of electrocatalysts for proton exchange membrane fuel cells. Int J Mol Sci 22: 3390.

68. Rakhshanpouri S, Rowshanzamir S (2013) Water transport through a PEM fuel cell in a seven-layer model Energy 50: 220-231.

69. Wang Y, Wang CY (2005) Simulation of flow and transport phenomena in a polymer electrolyte fuel cell under low-humidity operation J. Power Sources 147(1-2): 148-161.

70. Zhang X, Higier A, Zhang X, Liu H (2019) Experimental studies of effect of land width in PEM fuel cells with serpentine flow field and carbon cloth Energies 12: 471.

71. Nam JH, Kaviany M (2003) Effective diffusivity and water-saturation distribution in single and two-layer PEMFC diffusion medium. Int J Heat Mass Transfer 40(24): 4595-4611.

72. Meng H, Wang CY (2004) Electron transport in PEFCs. J Electrochem Soc 151(3): A358-A367.

73. Li X, Sabir I (2005) Review of bipolar plates in PEM fuel cells: flow-field designs. Int J Hydrogen Energy 30(4): 359-371.

74. Chen K S, Hickner MA, Noble DR (2005) Simplified models for predicting the onset of liquid water droplet instability at the gas diffusion layer/gas flow channel interface. Int J Energy Res 29 (12): 1113-1132.

75. Sorensen B, Spazzafumo G (2018) Hydrogen and Fuel Cells. Emerging Technologies and Application. New York.

76. Khatib FN, Wilberforce T, Ijaodola O, Ogungbemi E, El Hassan Z, et al. (2019) Material degradation of components in polymer electrolyte membrane (PEM) electrolytic cell and mitigation mechanisms: A re-view. Renew. Sust. Energ Rev 111: 1-14.

77. Doan TL, Lee HE, Shah SSH, Kim MJ, Kim CH, et al. (2021) A review of the porous transport layerin pol-ymer electrolyte membrane water electrolysis. Int J Energy Res 45: 14207-14220.

78. Zhang G, Jiao K (2018) Multi-phase models for water and thermal management of proton exchange membrane fuel cell: A re-view. J Power Sources 391: 120-133.

79. Zhang T, Wang P, Chen H, Pei P (2018) A review of automotive proton exchange membrane fuel cell degradation under start-stop operating condition. Appl Energy 223: 249-262.

80. Ren P, Pei P, Li Y, Wu Z, Chen D, et al. (2020) Degradation mechanisms of proton exchange membrane fuel cell under typical automotive operating conditions. Prog Energy Combust Sci 80: 100859.

81. Chen D, Michael A, Hickner MA, Agar E, Kumbur EC (2013) Optimized Anion Exchange Membranes for Vanadium Redox Flow Batteries. ACS Appl Mater Interfaces 5(15): 7559-7566.

82. Zhang Y, Zhong Y, Bian W, Liao W, Zhou X, et al. (2020) Robust proton exchange membrane for vanadium redox flow batteries reinforced by silica-encapsulated nanocellulose. Int J Hydrog Energy 45: 9803-9810.

83. Xue R, Jiang F, Wang F, Zhou X (2020) Towards cost-effective proton-exchange membranes for redox flow batteries: A fac-ile and innovative method. J Power Sources 449: 227475.

84. Huang CL, Kung YR, Shao YJ, Liou GS (2021) Synthesis and characteristics of novel TPA-containing electrochromic poly (ether sulfone) s with dimethylamino substituents. Electrochim. Acta 368: 137552.

85. Cichosz S, Masek A, Zaborski M (2018) Polymer-based sensors: A review. Polym Test 67: 342-348.

86. Grot WG (1982) Nafion® Membrane and its Applications. Boston.

87. Steck A (1995) in "Proceedings of the First International Symposium on New Materials for Fuel Cell Systems". Canada.

88. Tank MR, Darst KR, Lee KD, Martin CW (1989) in "Multiphase Polymers: Blends and Ionomers". Washington.

89. Watkins DS (1988) Canadian solid polymer fuel cell development in "Abstracts 33rd Int. Pennington.

90. Watkins DS (1983) in "Fuel Cell Systems". Plenum Press.

91. Prater K (1990) The renaissance of the solid polymer fuel cell. J Power Sources 29: 239-250.

92. Kienitz B, Kolde J, Priester S, Baczkowski C, Crum, M (2011) Ultra-thin reinforced ionomer membranes to meet next gen-eration fuel cell targets. ECS Trans 41: 1521-1530.

93. Mohammadi G, Jahanshahi M, Rahimpour A (2013) Fabrication and evaluation of Nafion nanocomposite membrane based on ZrO_2-TiO_2 binary nanoparticles as fuel cell MEA. Int J Hydrogen Energy 38: 9387-9394.

94. Ketpang K, Lee K, Shanmugam S (2014) Facile synthesis of porous metal oxide nanotubes and modified nafion composite membranes for polymer electrolyte fuel cells operated under low relative humidity. ACS Appl Mater Interfaces 6 (19): 16734-16744.

95. Taghizadeh MT, Vatanparast M (2017) Nafion/sulfonic acid functionalized SnO_2/SiO_2 nanocomposite for mitigation of mem-brane chemical degradation in PEM fuel cells. J Mater Sci Mater Electron 28: 778-786.

96. Xu G, Wu Z, Wei Z, Zhang W, Wu J, et al. (2020) non-destructive fabrication of Nafion/silica compo-site membrane via swelling-filling modification strategy for high temperature and low humidity PEM fuel cell. Renewable Energy 153: 935-939.

97. Liu F, Yi B, Xing D, Yu J, Zhang H (2003) Nafion/PTFE composite membranes for fuel cell applications. J Membr Sci 212: 213-223.

98. Yu TL, Lin HL, Shen KS, Huang LN, et al. (2004) Nafion/PTFE composite membranes for fuel cell applications. J Polym Res 11: 217-224.

99. Tang H, Wang X, Pan M, Wang F (2007) Fabrication and characterization of improved PFSA/ePTFE composite polymer elec-trolyte membranes. J Membr Sci 306: 298-306.

100. Jung GB, Weng FB, Su A, Wang JS, Leon Yu T, et al. (2008) Nafion/PTFE/silicate mem-branes for high-temperature proton exchange membrane fuel cells. Int J Hydrogen Energy 33: 2413-2417.

101. Lin HL, Chang TJ (2008) Preparation of Nafion/PTFE/$Z_r(HPO_4)^2$ composite membranes by direct impregnation method. J Membr Sci 325: 880-886.

102. Weng FB, Wang JS, Leon Yu T (2008) The study of PTFE/Nafion/Silicate membranes operating at low relative humidity and elevated temperature. J Chin Inst Chem Eng 39: 429-433.

103. Lin HL, Yeh SH, Yu TL, Chen LC (2009) Silicate and zirconium phosphate modified Nafion/PTFE composite mem-branes for high temperature PEMFC. J Polym Res 16: 519-527.

104. Yoon KR, Lee KA, Jo S, Yook SH, Lee KY, et al. (2019) Mussel-inspired polydopamine-treated rein-forced composite membranes with self-supported CeOx radical scavengers for highly stable PEM fuel cells. Adv Funct Mater 29: 1806929.

105. Zhang X, Trieu D, Zheng D, Ji W, Qu H, et al. (2021) Nafion/PTFE Composite Membranes for a High Temperature PEM Fuel Cell Application. Ind Eng Chem Res 60: 11086-11094.

106. Pletcher D, Walsh FC (1990) Industrial Electrochemistry. New York.

107. Liu C, Martin CR (1990) Ion Transporting Composite Membranes: II. Ion Transport Mechanism in Nafion-Impregnated Gore-Tex Membranes. J Electrochem Soc 137: 510.

108. Verbrugge MW, Hill RF, Schneider EW (1992) Composite membranes for fuel-cell applications. AIChE Journal 38: 93-100.

109. Zakil FA, Kamarudin SK, Basri S (2016) Modified Nafion membranes for direct alcohol fuel cells: An overview. Renewable and Sustainable Energy Reviews,Renewable Sustainable Energy Rev 65: 841-852.

110. Lee JS, Hwang IT, Jung CH, Choi JH (2016) Surface modification of Nafion membranes by ion implantation to reduce methanol crossover in direct methanol fuel cells. RSC Adv 6: 62467-62470.

111. Ng WW, Thiam HS, Pang YL, Chong KC, Lai SO (2022) A State-of-Art on the Development of Nafion-Based Membrane for Performance Improvement in Direct Methanol Fuel Cells. Membranes 12: 506.

112. Teixeira FC, Teixeira APS, Rangel CM (2022) New proton conductive membranes of indazole- and condensed pyra-zolebisphosphonic acid-Nafion membranes for PEMFC. Renewable Energy 196: 1187-1196.

113. Zhu LY, Li YC, Liu J, He J, Wang LY, et al. (2022) Recent developments in high-performance Nafion membranes for hydrogen fuel cells applications. Petroleum Sci 19: 1371-1381.

114. Shin SH, Kodir A, Shin D, Park SH, Bae B (2019) Perfluorinated composite membranes with organic antioxidants for chemically durable fuel cell. Electrochimica Acta 298: 901-909.

115. Mazzapioda L, Panero S, Navarra MA (2019) Polymer Electrolyte Membranes Based on Nafion and a Superacidic Inorganic Additive for Fuel Cell Applications. Polymers 11(5): 914.

116. Oh K, Kwon O, Son B, Lee DH, Shanmugam S (2019) Nafion-sulfonated silica composite membrane for proton ex-change membrane fuel cells under operating low humidity condition. J Membr Sci 583: 103-109.

117. Parnian MJ, Rowshanzamir S, Moghaddam JA (2018) Investigation of physicochemical and electrochemical properties of recast Nafion nanocomposite membranes using different loading of zirconia nanoparticles for proton exchange mem-brane fuel cell applications. Mater Sci Energy Technol 1: 146-154.

118. Choi J, Yeon JH, Yook SH, Shin S, Kim JY, et al. (2021) Multifunctional Nafion/CeO_2 Dendritic Structures for Enhanced Durability and Performance of Polymer Electrolyte Membrane Fuel Cells. ACS Appl Mater Interfaces 13(1): 806-815.

119. Vinothkannan M, Kim AR, Kumar GG, Yoo JD (2018) Sulfonated graphene oxide/Nafion composite membranes for high temperature and low humidity proton exchange membrane fuel cells. RSC Adv 8(14): 7494-7508.

120. Kannan R, Kakade BA, Pillai VK (2008) Polymer electrolyte fuel cells using Nafion-based composite membranes with func-tionalized carbon nanotubes, Angew Chem Int 47(14): 2653-2656.

121. Kannan R, Parthasarathy M, Maraveedu SU, Kurungot S, Pillai VK (2009) Domain size manipulation of perflouorinated polymer electrolytes by sulfonic acid-functionalized MWCNTs to enhance fuel cell performance, Langmuir 25: 8299-8305.

122. Cele NP, Sinha Ray S, Pillai SK, Ndwandwe M, Nonjola S, et al. (2010) Carbon nanotubes based nafion composite membranes for fuel cell applications. Fuel Cells 64-71.

123. Steffy NJ, Parthiban V, Sahu AK (2018) Uncovering Nafion-multiwalled carbon nanotube hybrid membrane for pro-spective polymer electrolyte membrane fuel cell under low humidity. J Membr Sci 563: 65-74.

124. (2022) for Durable Proton-Exchange Membrane Fuel Cells. Membranes 12: 1073.

125. Maiti J, Kakati N, Woo SP, Yoon YS (2018) Nafion® based hybrid composite membrane containing GO and dihydrogen phosphate functionalized ionic liquid for high temperature polymer electrolyte membrane fuel cell. Compos Sci Technol 155: 189-196.

126. Danyliv O, Martinelli A (2019) Nafion/Protic Ionic Liquid Blends: Nanoscale Organization and Transport Properties. J Phys Chem C 123: 14813-14824.

127. Fan L, Shi J, Xi Y (2020) PVDF-Modified Nafion Membrane for Improved Performance of MFC. Membranes 10(8): 185.

128. (2019) mem-brane induced by blending sulfonated poly (arylene ether ketones) for direct methanol fuel cells. J Membr Sci 573: 439-447.

129. Ru C, Gu Y, Duan Y, Na H, Zhao C (2019) Nafion based semi-interpenetrating polymer network membranes from a cross-linkable SPAEK and a fluorinated epoxy resin for DMFCs. Electrochim. Acta 324: 134873.

130. Mazinani V, Tabaian SH, Rezaei M, Mallahi M, Mohammadijoo M, et al. (2014) Synthesis and Characterization of Nafion-ZrOH-CaO Hybrid Membrane for Proton Exchange Membrane Fuel Cell. J Fuel Cell Sci Technol 11: 031004.

131. Ozden A, Ercelik M, Ozdemir Y, Devrim Y, Colpan CO (2017) Enhancement of direct methanol fuel cell performance through the inclusion of zirconium phosphate. Int. J Hydrog Energy 42: 21501-21517.

132. Sigwadi R, Dhlamini MS, Mokrani T, Nemavhola F, Nonjola PF, et al. (2019) The proton conductivity and mechani-cal properties of Nafion®/ ZrP nanocomposite membrane. Heliyon 5(8): e02240.

133. Prapainainar P, Du Z, Theampetch A, Prapainainar C, Kongkachuichay P, et al. (2019) Properties and DMFC per-formance of nafion/mordenite composite membrane fabricated by solution-casting method with different solvent ratio. Energy 190: 116451.

134. Sun X, Yang C, Xia Z, Qi F, Sun H, et al. (2020) Molecular sieve as an effective barrier for methanol crossover in direct methanol fuel cells. Int J Hydrog Energy 45: 8994-9003.

135. Cui Y, Baker AP, Xu X, Xiang Y, Wang L, et al. (2015) Enhancement of Nafion based membranes for direct methanol fuel cell applications through the inclusion of ammonium-X zeolite fillers. J Power Sources 294: 369-376.

136. Prapainainar P, Du Z, Kongkachuichay P, Holmes SM, Prapainainar C (2017) Mordenite/Nafion and analcime/Nafion composite membranes prepared by spray method for improved direct methanol fuel cell performance. Appl Surf Sci 421: 24-41.

137. Prapainainar P, Pattanapisutkun N, Prapainainar C, Kongkachuichay P (2018) Incorporating graphene oxide to improve the performance of Nafion-mordenite composite membranes for a direct methanol fuel cell. Int J Hydrog Energy 44: 362-378.

138. Cohen SG, Wolosinski HT, Scheuer P (1949) α, β, β-Trifluorostyrene and α-Chloro-β, β-difluorostyrene. J Am Chem Soc 71: 3439.

139. Hodgdon RB (1968) Polyelectrolytes Prepared from Perfluoroalkylaryl Macromolecules. J Polymer Science 6: 171-191.

140. Steck A, Stone C (1997) in "Proceedings of the Second International Symposium on New Materials for Fuel Cell and Modern Battery Systems. Canada.

141. Basura VI, Chuy C, Beattie PD, Holdcroft S (2001) Effect of equivalent weight on electrochemical mass transport properties of oxygen in proton exchange membranes based on sulfonated α, β, β-trifluorostyrene (BAM®) and sulfonated styrene-(ethylene-butylene)-styrene triblock (DAIS-analytical) copolymers. J Electroanal. Chem 501: 77-88.

142. Walkowiak Kulikowska J, Wolska J, Koroniak H (2017) "10. Polymers application in proton exchange membranes for fuel cells (PEMFCs)". Boston.

143. Biancolli AL, Bsoul Haj S, Douglin JC, Barbosa AS, Sousa RR, et al. (2022) High-performance radiation grafted anion-exchange membranes for fuel cell applications: Effects of irradiation condi-tions on ETFE-based membranes properties. J Membr Sci 641: 119879.

144. Chapiro A (1962) Radiation Chemistry of Polymeric Systems, High Polymers. New York.

145. Kerres J, Cui W, Eigenberger G, Bevers D, Schnurnberger W, et al. (1996) in "Proceedings of the 11th Hy-drogen Conference". Germany.

146. Scherer GG (1990) Polymer Membranes for Fuel Cells, Ber Bunsenges Phys Chem 94: 1008-1014.

147. Zhang H, Shen PK (2012) Recent Development of Polymer Electrolyte Membranes for Fuel Cells. Chem Rev 112(5): 2780-2832.

148. Kaplan BY, Kirlioglu AC, Jamil E, Yurum A, Rajabalizadeh N, et al. (2020) Radiation-Grafter Polymer Electrolyte Membranes for Fuel Cells. Hacettepe J Biol Chem 48 (5): 483-506.

149. Li X, Zhang H, Lin C, He Z, Ramani V (2022) Quantitative analysis of proton exchange membrane prepared by radiation-induced grafting on ultra-thin FEP film. Int J Hydrog Energy 47(3): 1874-1887.

150. Kim B, Weaver A, Chumakov M, Pazos IM, Poster DL, et al. (2018) Mechanisms and Characterization of the Pulsed Electron-Induced Grafting of Styrene onto Poly(tetrafluoroethylene-co-hexafluoropropylene) to Prepare a Polymer Electrolyte Membrane. Radiat Res 190(3): 309-321.

151. Kimura Y, Chen J, Asano M, Maekawa Y, Katakai R, et al. (2007) Anisotropic proton-conducting membranes prepared from swift heavy ion-beam irradiated ETFE films. Nucl Instrum Methods 263: 463.

152. Farquet P, Padeste C, Borner M, Ben Youcef H, Gursel SA, et al. (2008) Microstructured proton-conducting membranes by synchrotron-radiation-induced grafting. J Membr Sci 325: 658.

153. Biancolli ALG, Herranz D, Wang L, Stehliková G, Soualhi RB, et al. (2018) ETFE-based anion-exchange membrane ionomer powders for alkaline membrane fuel cells: a first performance comparison of head-group chemistry. J Mater Chem A 6(47): 24330- 24341.

154. Ke X, Drache M, Gohs U, Kunz U, Beuermann S (2018) Preparation of Polymer Electrolyte Membranes via Radiation-Induced Graft Copolymerization on Poly(ethylene-alt-tetrafluoroethylene) (ETFE) Using the Crosslinker N, N′-Methylenebis(acrylamide). Membranes 8(4): 102.

155. Ke X, Zhang Y, Gohs U, Drache M, Beuermann S (2019) Polymer Electrolyte Membranes Prepared by Graft Copolymerization of 2-Acrylamido-2-Methylpropane Sulfonic Acid and Acrylic Acid on PVDF and ETFE Activated by Electron Beam Treatment. Polymers 11(7): 1175.

156. Hao LH, Tap TD, Hieu DTT, Korneeva E, Tiep, et al. (2021) Morphological characterization of grafted polymer electrolyte membranes at a surface layer for fuel cell application. J Appl Polym Sci 139(4).

157. Yamaki T, Asano M, Maekawa Y, Morita Y, Suwa T, et al. (2003) Radiation grafting of styrene into crosslinked PTFE films and subsequent sulfonation for fuel cell applications. Radiat Phys. Chem 67: 403-407.

158. Sawada S, Yamaki T, Nishimura H, Asano M, Suzuki A, et al. (2008) Water transport properties of crosslinked-PTFE based electrolyte membranes. Solid State Ion 179(27): 1611-1614.

159. Yamaki T, Sawada S, Asano M, Maekawa Y, Youshida M, et al. (2009) Fuel-Cell Performance of Multiply-Crosslinked Polymer Electrolyte Membranes Prepared by Two-Step Radiation Technique. ECS Trans 25(1): 1439.

160. Sawada S, Yamaki T, Kawahito S, Asano M, Suzuki, et al. (2009) Thermal stability of proton exchange fuel-cell membranes based on crosslinked-polytetrafluoroethylene for membrane-electrode assembly preparation. Polym Degrad. Stab 94(3): 344-349.

161. Muto F, Oshima A, Kakigi T, Mitani N, Matsuura A, et al. (2007) Synthesis and characterization of PEFC membranes based on fluorinated-polymer-alloy using pre-soft-EB grafting method. Nucl Instrum Methods Sect B 265(1): 162-167.

162. Asano M, Chen J, Maekawa Y, Sakamura T, Kubota H, et al. (2007) Novel UV-induced photografting process for preparing poly(tetrafluoroethylene)-based proton-conducting membranes. J Polym Sci A: Polym. Chem 45(13): 2624-2637.

163. Dargaville TR, George GA, Hill DJT, Whittaker AK (2003) High energy radiation grafting of fluoropolymers, Prog. Polym Sci 28 1355-1376.

164. Yoshida M, Kimura Y, Chen J, Asano M, Maekawa Y (2009) Preparation of PTFE-based fuel cell membranes by combining latent track formation technology with graft polymerization. Radiat Phys Chem 78(12): 1060-1066.

165. Feng S, Zhong Z, Wang Y, Zing W, Drioli E (2018) Progress and perspectives in PTFE membrane: Preparation, modification, and applications. J Memb Sci 549: 332-349.

166. Sasa D, Sinirlioglu D, Muftuoglu AE, Eren F, Celik SU, et al. (2013) Synthesis and characterization of 1H-1,2,4-triazole functional polymer electrolyte membranes (PEMs) based on PVDF and 4-(chloromethyl) styrene via photoinduced grafting. J Polym Res 20(12): 313.

167. Golcuk S, Muftuoglu AE, Celik SU, Bozkurt A (2013) Synthesis and characterization of polymer electrolyte membranes based on PVDF and styrene via photoinduced grafting. J Polym Res 20(5): 144.

168. Sadeghi S, Şanlı LI, Güler E, Gürsel SA (2018) Enhancing proton conductivity via sub-micron structures in proton conducting membranes originating from sulfonated PVDF powder by radiation-induced grafting, Solid State Ion 314 66-73.

169. Tahrim AA, Amin INHM (2019) Advancement in Phosporic Acid Doped Polybenzimidazole Membrane for High Temperature PEM Fuel Cells: A review. JAMST 23: 37-62.

170. Chen H, Wang S, Liu F, Wang D, Wang Z. et al. (2019) Base-acid doped polybenzimidazole with high phosphoric acid retention for HT-PEMFC applications. J Mem Sci 596: 117722.

171. He RH, Li Q, Xiao G, Bjerrum NJ (2003) Proton conductivity of phosphoric acid doped polybenzimidazole and its composites with inorganic proton conductors. J Mem Sci 226: 169-184.

172. Samms SR, Wasmus S, Savinell RF (1996) Thermal Stability of Proton Conducting Acid Doped Polybenzimidazole in Simulated Fuel Cell Environments. J Electrochem Soc 143 1225.

173. Wang J, Wasmus S, Savinell RF (1995) Evaluation of Ethanol, 1-Propanol, and 2-Propanol in a Direct Oxidation Polymer-Electrolyte Fuel Cell: A Real-Time Mass Spectrometry Study. J Electrochem Soc 142: 4218.

174. Wang J, Savinell RF, Wainright J, Litt M, Yu H (1996) A H2O2 fuel cell using acid doped polybenzimidazole as polymer electrolyte. Electroch. Acta 41 193-197.

175. Wainright J, Savinell RF, Litt M (1997) Proceedings of the Second International Symposium on New Materials for Fuel Cell and Modern Battery Systems, Eds. O. Savadogo and P.R. Roberge, Montréal, Canada, July 6-10 p. 808.

176. Maity S, Singha Ss, Jana T (2015) Low acid leaching PEM for fuel cell based on polybenzimidazole nanocomposites with protic ionic liquid modified silica. Polymer 66: 76-85.

177. Özdemir Y, Özkan N, Devrim Y (2017) Fabrication and Characterization of Cross-linked Polybenzimidazole Based Membranes for High Temperature PEM Fuel Cells. Electrochimica Acta 245: 1-13.

178. Wang L, Ni J, Liu D, Gong C, Wang L (2018) Effects of branching structures on the properties of phosphoric acid-doped polybenzimidazole as a membrane material for high-temperature proton exchange membrane fuel cells. Int J Hydrog Energy 43: 16694-16703.

179. Haque MA, Sulong AB, Majlan EH, Loh KS, Husaini T, Rosli R (2019) Physiochemical Characteristics of Solid Electrolyte Membranes for Hight-Temperature PEM Fuel Cell. Int J Electrochem. Sci 14: 371-386.

180. Seng LK, Masdar MS, Shyuam LK (2021) Ionic Liquid in Phosphoric Acid-Doped Polybenzimidazole (PA-PBI) as Electrolyte Membranes for PEM Fuel Cells: A Review. Membranes 11(10): 728.

181. Gao C, Hu M, Wang L, Wang L (2020) Synthesis and properties of phosphoric-acid-doped polybenzimidazole with hyperbranched cross-linkers decorated with imidazolium groups as high-temperature proton exchange membranes. Polymers 12(3): 515.

182. Liu F, Wang S, Chen H, Li J, Tian X, et al. (2018) Cross-linkable polymeric ionic liquid improves phosphoric acid retention and long-term conductivity stability in polybenzimidazole based PEMs. ACS Sustain. Chem Eng 6: 16352-16362.

183. Liu F, Wang S, Chen H, Li J, Wang X, et al. (2021) The impact of poly (ionic liquid) on the phosphoric acid stability of polybenzimidazole-base HT-PEMs. Renew. Energy 163: 1692-1700.

184. Escorihuela J, Sahuquillo O, Bernabé AG, Gimenez E, Compan V (2018) Phosphoric Acid Doped Polybenzimidazole (PBI)/Zeolitic Imidazolate Framework Composite Membranes with Significantly Enhanced Proton Conductivity under Low Humidity Conditions. Nanomaterials 8: 775.

185. Rajabi Z, Javanbakht M, Hooshyari K, Adibi, M Badiei A (2021) Phosphoric acid doped polybenzimidazole based polymer electrolyte membrane and functionalized SBA-15 mesoporous for elevated temperature fuel cell. Int J Hydrog Energy 46: 33241-33259.

186. Cornet N, Diat O, Gebel G, F Jousse F, D Marsacq D, Mercier R, Pineri, M (2000) Sulfonated polyimide membranes: a new type of ion-conducting membrane for electrochemical applications. J New Mat Electrochem. Systems 3: 33-42.

187. Woo Y, Young Oh S, Kang YS, Jung B (2003) Synthesis and characterization of sulfonated polyimide membranes for direct methanol fuel cell. J Membr Sci 220: 31-45.

188. Zhai F, Guo X, Fang J, Xu H (2007) Synthesis and properties of novel sulfonated polyimide membranes for direct methanol fuel cell application. J Membr Sci 296: 102-109.

189. You PY, Kamarudin SK, Masdar MS (2019) Improved performance of sulfonated polyimide composite membranes with rice husk ash as a biofiller for application in direct methanol fuel cells. Int J Hydrogen Energy 44: 1857-1866.

190. Hu M, Zhang B, Chen J, Xu M, Liu D, Wang L (2019) Cross-linked polymer electrolyte membrane based on a highly branched sulfonated polyimide with improved electrochemical properties for fuel cell applications. Int J Energy Res 43: 8753-8764.

191. Wnek GE, Rider JN, Serpico JM, Einset AG, Ehrenberg SG, Raboin L (1995) in Proceedings of the First International Symposium on Proton Conducting Membrane Fuel Cells. The Electrochemical Society Proceedings, Eds. Gottesfeld S Halpert G., and Landgrebe A 95-23, 247.

192. Park HS, Hong CK (2021) Anion Exchange Membrane Based on Sulfonated Poly (Styrene-Ethylene-Butylene-Styrene) Copolymers. Polymers 13(10): 1669.

193. Juanes RT, Río C, Gil Castell O, Primaz C, Ribes Greus A (2021) Triblock SEBS/DVB crosslinked and sulfonated membranes: Fuel cell performance and conductivity. J Appl Polym Sci 138: 50671.

194. Hale WF, Farnham AG, Johnson RN, Clendinning RA (1967) Poly (Aryl ethers) by nucleophilic aromatic substitution. II. Thermal stability. J Poly Sci A-1 5: 2399.

195. Johnson RN (1969) in "Encyclopedia of Polymer Science and Technology". New York.

196. Lade H, Kumar V, Arthanareeswaran G, Ismail AF (2017) Sulfonated poly (arylene ether sulfone) nanocomposite electrolyte membrane for fuel cell applications: A review. Int J Hydrog Energy 42: 1063-1074.

197. Xu M, Xue H, Wang Q, Jia L (2021) Sulfonated poly (arylene ether) s-based proton exchange membranes for fuel cells. Int J Hydrog Energy 46: 31727-31753.

198. Kim K, Heo P, Hwang W, Baik JH, Sung YE, Lee JC (2018) Cross-Linked Sulfonated Poly (arylene ether sulfone) Containing a Flexible and Hydrophobic Bishydroxy Perfluoropolyether Cross-Linker for High-Performance Proton Exchange Membrane. ACS Appl Mater Interfaces 10 26: 21788-21793.

199. Choi J, Kyeong M, Kim M, Lee SS, Seo B Park, et al. (2021) Synthesis of Sulfonated Poly (Arylene Ether Sulfone) s Containing Aliphatic Moieties for Effective Membrane Electrode Assembly Fabrication by Low-Temperature Decal Transfer Methods. Polymers 13(11): 1713.

200. Kim JH, Vinothkannan M, Kim AR, Yoo DJ (2020) Anion Exchange Membranes Obtained from Poly (arylene ether sulfone) Block Copolymers Comprising Hydrophilic and Hydrophobic Segments. Polymers 12: 325.

201. Schmeller A, Ritter H, Ledjeff K, Nolte R, Thorwirth R (1993) Polymer Electrolyte Membrane and Process for The Production.

202. Zhao C, Li X, Wang Z, Dou Z, Zhong S (2006) Synthesis of the block sulfonated poly (ether ether ketone) s (S-PEEKs) materials for proton exchange membrane. J Memb Sci 280: 643-650.

203. Wong CY, Wong WY, Ramya K, Khalid M, Loh KS, et al. (2019) Additives in proton exchange membranes for low and high-temperature fuel cell applications: A review. Int J Hydrog Energy 44: 6116-6135.

204. Xu M, Xue H, Wang Q, Jia L (2021) Sulfonated poly (arylene ether) s-based proton exchange membranes for fuel cells. Int J Hydrog Energy 46: 31727-31753.

205. Parnian MJ, Rowshnamir S, Gashoul F (2017) Comprehensive investigation of physicochemical and electrochemical properties of sulfonated poly (ether ether ketone) membranes with different degrees of sulfonation for proton exchange membrane fuel cell applications. Energy 125: 614-628.

206. Sun CY, Zhang H, Luo XD, Chen N (2019) A comparative study of Nafion and sulfonated poly (ether ether ketone) membrane performance for iron-chromium redox flow battery. Ionics 25: 4219-4229.

207. Wu Y, He G, WuX, Yuan Q, Gong X, et al. (2019) Confinement of functionalized graphene oxide in sulfonated poly (ether ether ketone) nanofibers by coaxial electrospinning for polymer electrolyte membranes. Int J Hydrog Energy 44: 7494-7504.

208. Pasquini L, Zhakisheva B, Sgreccia E, Narducci R, Di Vona ML, et al. (2021) Stability of Proton Exchange Membranes in Phosphate Buffer for Enzymatic Fuel Cell Application: Hydration, Conductivity and Mechanical Properties. Polymers 13(3): 475.

209. Herrmann WO, Haehnel W (1924) Chem. Forschungsgemeinschaft; DE-OS 450 286; American Chemical Society: USA.

210. Herrmann WO, Haehnel W, Berg H (1937) Chem. Forschungsgemeinschaft, DE642531. Chem Abstr 31: 59059.

211. Sapalidis AA (2020) Porous Polyvinyl Alcohol Membranes: Preparation Methods and Applications. Symmetry 12 960.

212. Pivovar BS, Wang Y, Cussler EL (1999) Pervaporation membranes in direct methanol fuel cells. J Memb Sci 154 155-162.

213. Maiti J, Kakati N, Lee SH, Viswanathan B, Yoon YS (2012) Where Do Poly (Vinyl Alcohol) Based Membranes Stand in Relation to Nafion® for Direct Methanol Fuel Cell Applications? J Power Sources 216: 48-66.

214. Bolto B, Tran T, Hoang M, Xie Z (2009) Crosslinked poly (vinyl alcohol) membranes. Prog Polym Sci 34: 969-981.

215. Truong YB, Choi J, Mardel J, Gao Y, Maisch S, et al. (2017) Functional Cross-Linked Electrospun Polyvinyl Alcohol Membranes and Their Potential Applications. Macromol Mater Eng 302: 1700024.

216. Wong CY, Wong WY, Loh KS, Daud WRW, Lim KL, et al. Development of Poly (Vinyl Alcohol)-Based Polymers as Proton Exchange Membranes and Challenges in Fuel Cell Application: A Review, Polymer Reviews 60(1): 171-202.

217. Rhim JW, Park HB, Lee CS, Jun JH, Kim DS, Lee YM (2004) Crosslinked poly (vinyl alcohol) membranes containing sulfonic acid group: proton and methanol transport through membranes. J Memb Sci 238: 143-151.

218. Hou Y, Li K, Luo H, Liu G, Zhang R, et al. (2013) Using Crosslinked Polyvinyl Alcohol Polymer Membrane as a Separator in the Microbial Fuel Cell. Front Environ Sci Eng 8: 137-143.

219. Seeponkai N, Wootthikanokkhan J (2007) Proton Conductivity and Methanol Permeability of Sulfonated Poly (Vinyl Alcohol) Membranes Modified by Using Sulfoacetic Acid and Poly (Acrylic Acid). J Appl Polym Sci 105: 838-845.

220. Zakaria Z, Kamarudin SK (2020) A review of quaternized polyvinyl alcohol as an alternativepolymeric membrane in DMFCs and DEFCs. Int J Energy Res 44: 6223-6239.

221. Kumar SR, Juan CH, Lia GM, Lin JS, Yang CC, et al. (2016) Fumed silicananoparticles incorporated in quaternized poly (vinyl alcohol) nanocomposite membrane for enhanced power densities indirect alcohol alkaline fuel cells. Energies 9: 15.

222. Lin JS, Kumar SR, Ma WT, Shih CM, Teng LW, et al. (2017) Gradiently distributed ironoxide@ graphene oxide nanofillers in quaternized polyvinylalcohol composite to enhance alkaline fuel cell power density. J Membr Sci 543: 28-39.

223. Gouda MH, Gouveia W, Afonso ML, Šljukić B, Essawy NA, et al. (2019) Poly (vinyl alcohol)-based crosslinked ternary polymer blend doped with sulfonated graphene oxide as a sustainable composite membrane for direct borohydride fuel cells. J Power Sources 432: 92-101.

224. Gouda MH, Elessawy NA, Toghan A (2021) Novel Crosslinked Sulfonated PVA/PEO Doped with Phosphated Titanium Oxide Nanotubes as Effective Green Cation Exchange Membrane for Direct Borohydride Fuel Cells. Polymers 13: 2050.

225. Zakaria Z, Kamarudin SK, Timmiati SN, Masdar MS (2019) New composite membrane poly (vinyl alcohol)/graphene oxide for direct ethanol-proton exchange membrane fuel cell. J Appl Polym Sci 136: 46928.

226. Ding C, Qiao Z (2022) A review of the application of polyvinyl alcohol membranes for fuel cells. Ionics 28: 1-13.

227. Choudhury RR, Gohil JM, Dutta K (2021) Poly (vinyl alcohol)-based membranes for fuel cell and water treatment applications: A review on recent advancements. Polym Adv Technol 32: 4175-4203.

228. Samsudin AM, Bodner M, Hacker VA (2022) Brief Review of Poly (Vinyl Alcohol)-Based Anion Exchange Membranes for Alkaline Fuel Cells. Polymers 14(17): 3565.